A POSSIBLE ELECTRICAL EQUIVALENT CIRCUIT FOR THE ELECTRO-ODOCELL

by:

GÜRSÜZ ÇELEBİ

Advisor:

PROF. NECMİ N. TANYOLAÇ

Department of Electrical Engineering

School of Engineering

Robert College

Bebek, Istanbul, Turkey

May 1967

ACKNOWLEDGEMENT

This thesis has been prepared for the partial fulfilment of the requirements of the Robert College School of Engineering.

It is a report on part of the investigation and experimentation with the Electro-odocell - an objective odor-measuring device being developed since 1964, in Robert College Research Center - in an effort to find a possible electrical equivalent circuit for its functional mechanism.

Bu tezin hazırlanmasına yardımcı pek değerli fikir ve desteklerinden ötürü sayın Prof. Necmi Tanyolaç'a sonsuz teşekkürlerimi sunarım.

Ayrıca, hesapların programlanmasındaki yardımlarından ötürü sayın Y. Müh. Gültekin Yıldız'a, dil üzerindeki düzeltmelerinden ötürü Miss Carol LaMotte'a, şekillerin çizimindeki yardımlarından ötürü Bay Demir Tiryakioğlu'na, baskıdaki yardımlarından ötürü Bayan Seval Gürel ve deneylerde kullanılan mekanik parçaların imâlinde pek çok emeği geçen sayın Yüsuf Sakallı'ya da sonsuz teşekkürlerimi bildiririm.

Gürbüz Çelebi

Mayıs 1967, İstanbul

CONTENTS

CHAPTER I

INTRODUCTION

Following is a report on part of the research work going on at Robert College Research Center, under the supervision of Prof. Dr. Necmi N. Tanyolaç.

The aim of this research has been to develop an objective odor-measuring instrument to replace the human nose in the detection and measurement of odor.

Research on the development of an objective odor-measuring instrument has been intensified since 1949 (1). Odocell developed at Purdue University in 1948 by Tanyolaç and Eaton was used by various investigators (2,3,4,5,6) for odor studies. Hartman(10) at Cornell University, Dravnieks (11) at IIT, Moncrieff (12) in England and Barton (15) in France had developed instruments to be used as objective odor-measuring devices.

In 1964, Tanyolaç presented the Electro-odocell as an instrument to detect and measure odor or micro-micro amounts of material in the air (16,17,18).

The basic concept attributed to the operation of the Electro-odocell is given in the following definition of odor made by Dr. J.R. Eaton and Dr. N.N. Tanyolaç (18):

"..theoretically all the materials available have odor and odor is due to the molecules given off by the odorants at normal temperature and pressure, and the molecular structure plays a major part in olfaction."

The principle of operation of the Electro-odocell has been described by Dr. Tanyolaç as follows (18):

"The Electro-odocell detects and measures the change in potential or current on a dielectric when one surface of the dielectric is contaminated by the molecules given off by odorants. The Electro-odocell is made of three parts. Fig.1.1

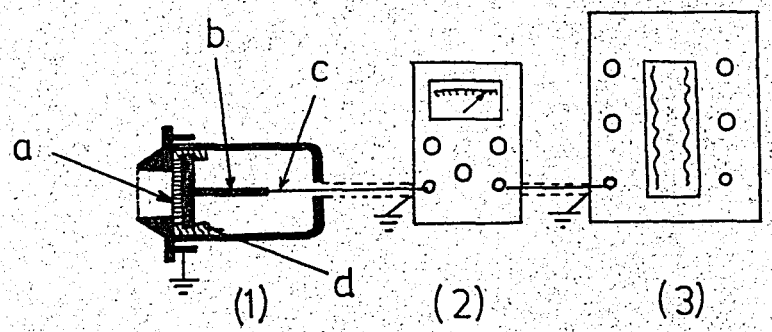

Fig. 1.1

Part one is a detector-transducer which has a surface sensitive to the molecules of materials and produces a change in voltage on the detector, depending on the type and amount of molecules absorbed on its surface. The sensitive surface of the detector (a) is open to the odor molecules and is made of dielectric materials, like mica, glass, plastics, paper, etc. The conducting surface of the detector (b) is covered with a copper or silver plate which is connected to a cable (c) well insulated from outside leakage and static charges. (d) is an insulation between metal plate and ground.

Part two is a micro-voltmeter which can record the voltage changes in the detector.

Part three is an automatic recorder which records the indication of the micro-voltmeter as a microvolts-versus-time curve".

The aim of this thesis is to find an electrical equivalent circuit of the Electro-odocell and investigate the effects of circuit constants on the detector sensitivity.

In Chapter II, the physical properties of the transducer, the recorded data from odor measurements and the properties of the measuring devices are covered.

Chapter III is concerned with the determination of transducer constants with reference to an electrical representation, namely the transducer resistance and capacitance.

Finally, Chapter IV is devoted to the mathematical representation of response curves for assumed inputs to the selected equivalent circuit. Some constants are defined here with reference to input functions, which are to be considered characteristic of a given odorant.

Chapter V summarizes the main conclusions of the thesis.

REFERENCES:

1. TANYOLAÇ, N.N. Study of Odors Ph.D. Thesis, Purdue University (1949)

2. TANYOLAÇ, N.N. and J.R. EATON. Study of Odors, Journal of the American Pharmaceutical Association, Scientific edition, Vol. XXXIX, No. 10, October 1950.

3. CAMPBELL, J.A., Z.F. AHMED, J.E. CHRISTIAN and J.R. EATON. A Study in the Measurements of Odors and the Deodorizing Effects of Certain Materials, Journal of the American Pharmaceutical Association, Scientific edition, Vol. XLII, No. 4, April 1953.

4. AHMED, Z.F., J.A. CAMPBELL, J.E. CHRISTIAN and J.R. EATON A Proposed Method for Determining the Effect of Deodorants on the Elimination of Alcohol Breath, Journal of the American Pharmaceutical Association, Scientific Edition, Vol. XLII, No. 4, April 1953.

5. EATON, J.R., J.E. CHRISTIAN and J.A. CAMPBELL. Rapid Surface Tension Determination Using a Modified Pendant Drop Technique, Journal of the American Pharmaceutical Association, Scientific Edition, Vol. XLIV, No. 8, August 1953.

6. EATON, J.R., J.E. CHRISTIAN and J.A. CAMPBELL. Surface Phenomena Related to Odor Measurements, Annals of the New York Academy of Sciences, Vol.58, Art.2. Basic Odor Research Correlation.

7. CHAPMAN, C.R., J.R. EATON. Electric Potential Changes at Surfaces as a Means of Measuring Odorous Atmospheric Contamination. AIEE Conference paper CP56-97.

8. KOPPLIN, J.O., J.R. EATON and J.E. CHRISTIAN, Studies on the Adsorption of Odorous Materials I. Surface Potential Changes of Solid and Liquid Absorbing Surfaces. Journal of the American Pharmaceutical Association, Scientific Edition, Vol. XLVIII, No.8 August 1959.

9. KOPPLIN, J.O., J.R. EATON and J.E. CHRISTIAN, Surface Potential Changes due to the Adsorption of Alcohol Vapors, Journal of the American Pharmaceutical Association, Scientific Edition, Vol. XLVIII, No.9 September 1959.

10. HARTMAN, J.D. and E.W. Tolle, An Apparatus Designed for the Electrochemical Estimation of Flavors in Vegetables, Food Technology, 1957, Vol. XI, No. 2, p.130-132.

11. DRAVNIEKS, A.A. ARF Lays Groundwork for Synthetic Nose, C&En April 3, 1961.

12. MONCRIEFF, R.W. An Instrument for Measuring and Classifying Odors, Journal of Applied Physiology, Vol.16, No.4, July 1961.

13. GRANZEIER, F.J. Chemo-Electric Odor Detection, Industrial Research, July-August 1962.

14. AMOORE, J.E., J.W. JOHNSTON,JR. and MARTIN RUBIN, The Stereochemical Theory of Odor, Scientific American, February 1964.

15. KUEHNER, R.L. Recent Advances in Odor: Theory, Measurement and Control, Annals of the New York Academy of Sciences, Vol.116, Art.2, July 30, 1964.

16. Patent No. 12287 of Turkish Ministry of Industry on Electro-Odocell.

17. TANYOLAÇ, N.N. Electro-Odocell for Odor Measurement, International Rhinology, Vol. III, No.3, January 1965.

18. TANYOLAÇ, N.N. The Electro-Odocell for Odor Measurement and Surface Effects. In the book of J.I. BREGMAN and A. DRAVNIEKS, Surface Effects in Detection, Spartan Books, Inc., 1965, pp. 89-102.

CHAPTER II

PROPERTIES OF DETECTOR AND MEASURING DEVICES

2.1 DETECTOR PROPERTIES:

The main feature and the principle of operation of the odor detector were explained in the previous chapter. Here we consider the internal properties of the transducer and the measuring devices as they are coupled to each other in a typical odor measurement experiment.

The dielectric of the transducer as it is held between the two conductors, is the molecule sensitive element. When the molecules of an odorant reach on one side of this dielectric, they produce a potential difference across it.

A dielectric can be represented by an equivalent circuit as shown in Fig.2.1.

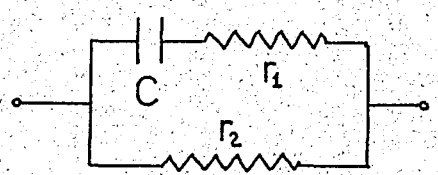

Fig 2.1

This conception of the dielectric takes into account the normal properties of the dielectric at voltages below its electric rupturing strength. Here the capacitor C represents the permittance and the resistance r_1 represents the dielectric absorbtion loss, the resistance r_2 represents the leakage component. In a perfect dielectric, r_1 would be zero and r_2 would be infinite. These two resistances can be combined in a single resistance placed either in series or in parallel with C, if the single resistance is properly proportioned.(1)

---

(1) KNOWLTON, A.E. Standard Handbook for Electrical Engineers p. 4-359

As will be seen in Chapter III and later in Chapter IV, it is important to adopt an equivalent circuit of the dielectric in trying to find an analogue for the odor measuring circuit, due to the fact that one has to take into account the input resistance and capacitance of the measuring instrument as compared to the internal resistance and capacitance of the detector.

Since in the case of the Electro-odocell, a dielectric is associated with an active element, it seems likely that we are confronted with for example a voltage generator of high internal resistance. In such a case to obtain accurate measurements of the detector output, a voltmeter of high input resistance should be used.

As will be seen from the results of experiments in Chapter III, the order of the dielectric resistance is around 10^9 ohms and its capacitance is around 200 pF for mica.

2.2 INSTRUMENT INPUT PROPERTIES:

As has been noted in the previous section the measuring instrument coupled to a high impedance source should have a high input impedance. In our measurements with the Electro-odocell a Model 610 B Electrometer fo Keithley Instruments, Inc. was used on its high input resistance (10^{14}ohms) voltage range.

This electrometer provides an output of $\pm$ 3 volts with a low internal impedance, which can be connected to a recorder. We also used an oscillographic recorder to see the shapes of the outputs. A Hewlet Packard Model 7701 A Recorder with a Model 8803 A High Gain DC Amplifier was used for this purpose.

In the voltmeter-ammeter measurements of dielectric resistance the same electrometer was used on its current range with a

Heathkit Regulated High Voltage Supply.

Capacitance was measured on a Type 1650-A Impedance Bridge by General Radio Company.

2.3 OUTPUT CHARACTERISTICS:

The circuit used to measure and record the output from the Electro-odocell at the same time is illustrated in Fig 2.2

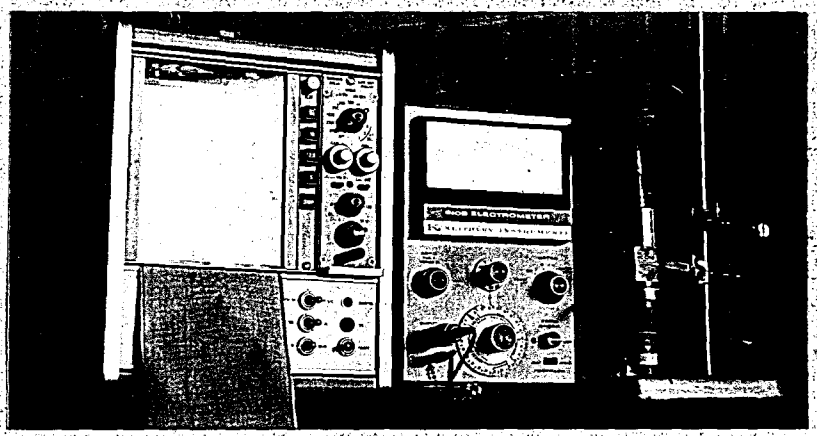

Fig 2.2

Generally the electrometer indicates a high voltage on a large scale before any odor is introduced. This may be attributed to the initial charges on the dielectric surface due to previous contact with air. The pressure of the transducer conductor plates on the dielectric also has a great effect on this initial voltage.

To be able to read smaller changes after the odorant has been introduced, and thus to increase the electrometer sensitivity, this initial voltage may be suppressed internally.

The polarity of voltages recorded from several odorants differ. For instance Acetone gives a negative output. It should be noted however that the polarity of output does not affect the scheme of analysis followed in dealing with input functions in Chapter IV. If a positive output has been assumed in the analysis whereas the actual output is negative, the introduction of the

negative sign in the final step will meet the actual requirements.

Fig 2.3 illustrates the most frequent output recordings obtained with several different odorants.

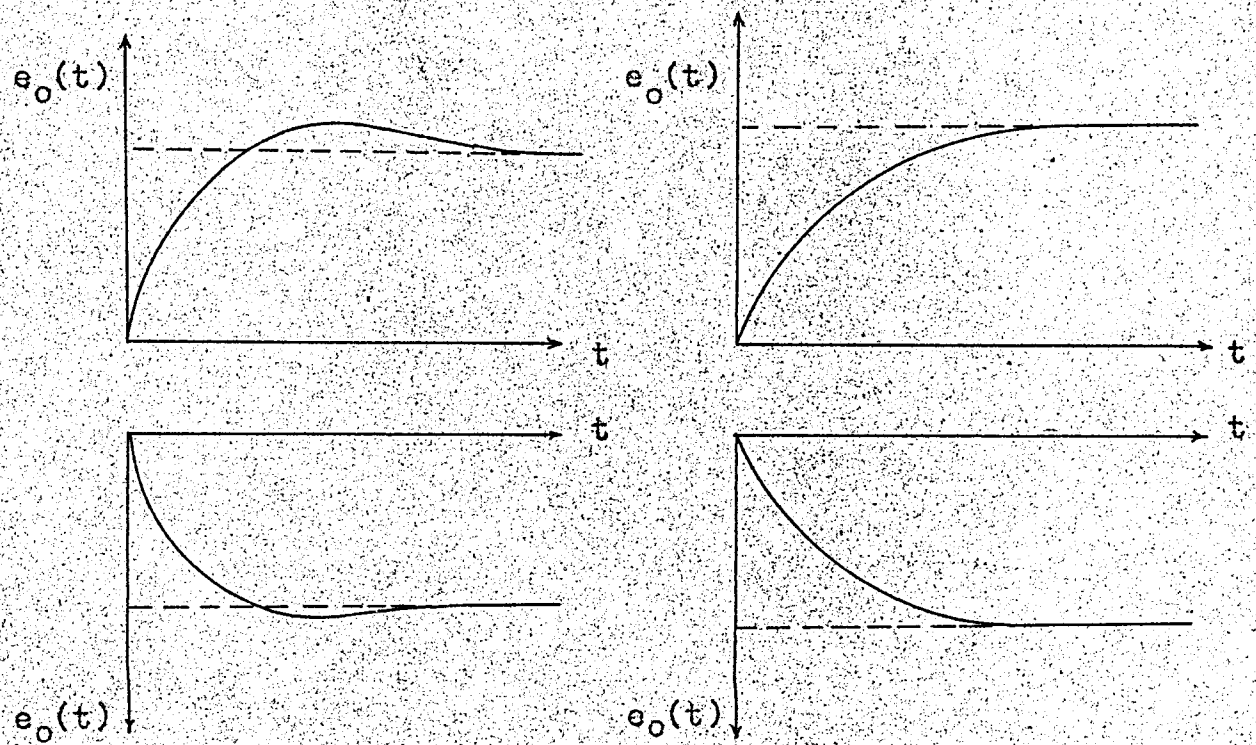

CHAPTER III

MEASUREMENTS:

3.1 RESISTANCE AND CAPACITANCE MEASUREMENTS

As will be seen in Chapter IV, the transducer and the measuring devices can be represented in an equivalent circuit, the elements of which involve the internal impedance and voltage source of the transducer and the input impedance of the measuring device. In this chapter, we shall attempt to determine the internal resistance and capacitance associate with the transducer. For this two approaches can be adopted;

1. Theoretical Calculations (from dielectric properties)
2. Direct Measurements

3.2 DIELECTRIC RESISTANCE:

In Chapter II the equivalent circuit of a dielectric was given by Fig 2.1, and it was also stated that for a perfect dielectric; $r_1 = 0$ and $r_2 = \infty$.

For the arrangement of the Electro-odocell, we may speak of two resistances which make up the total dielectric resistance r_2(1). This follows from the possible conditions of the current flow through the the dielectric. The two resistances, namely the s u r f a c e and the b u l k resistances can be represented as in Fig 3.1. The actual physical conditions and the electrical

---

(1) Here another resistance of question would be the resistance of the leakage path through the insulation resistance which is in contact with both, the high and low potential terminals. However, when the resistance of the whole transducer without the detector dielectric was measured, it was found that the insulation resistance was so high that it could be neglected in parallel with the detector dielectric resistance.

equivalent can be compared in that figure as follows:

In Fig 3.1a, horizontal arrows denote the current flow through the surface of the dielectric and vertical arrows denote the current flow through the volume.

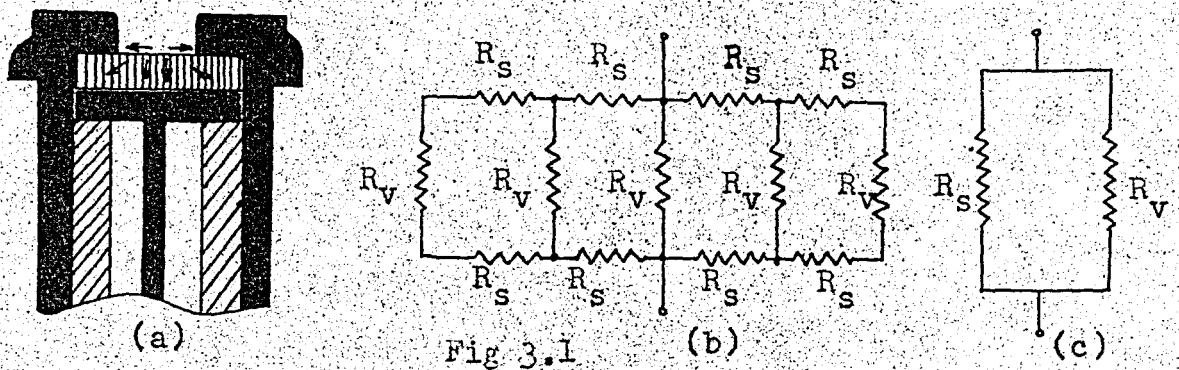

Fig 3.1

Here it is assumed that a high potential exists at the center of the open surface of the dielectric (since maximum charge can be collected at the center due to geometrical reasons) and surface currents if any, will flow radially outward to the ground conductor. In Fig 3.1b, the surface and the volume resistances for all the current paths are shown. Finally all these resistances can be combined into one s u r f a c e and one v o l u m e resistance. Fig 3.1c.

Based on the assumption of Fig 3.1c, experiments were conducted first to calculate the theoretical value of the total resistance and then to measure it by direct methods.

Theoretical Calculations:

Theoretical calculation of any resistance involves the determination of the resistivity of the given material and its geometry. For the dielectric of the Electro-odocell (EOC), two resistivities, namely the surface and the volume resistivities are necessary to calculate the total resistance.

"Volume resistivity of a material is the ratio of the potential gradient parallel to the current in the material, to the current density" and the "Surface Resistivity of a material is the ratio of the potential gradient parallel to the current along its surface to the current per unit width of resistance." (2)

V o l u m e R e s i s t i v i t y: Volume resistivity measurements were made according to ASTM Designation D 257-61, using the ammeter-voltmeter method with the precautions and equipment specified therin. (3)

The circuit diagram of the setup is given in Fig. 3.2 for measurements of volume resistivity.

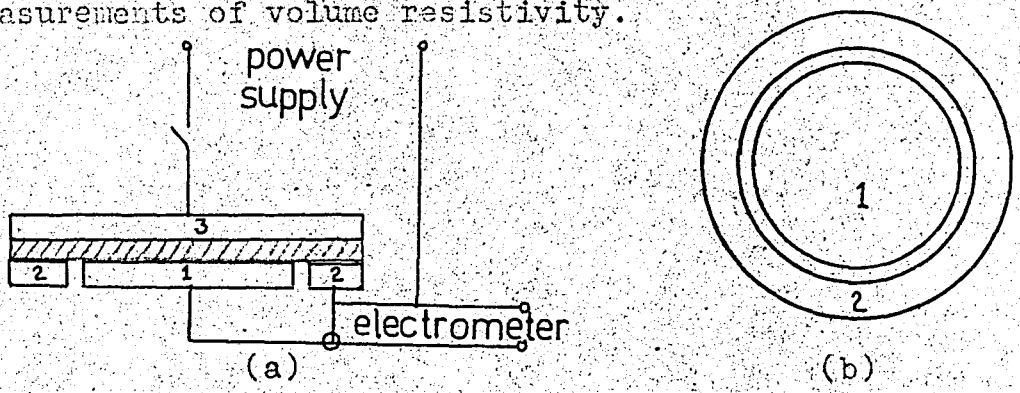

Fig 3.2

Electrode No.1 is called the guarded electrode, electrode No.2, the guard electrode and electrode No.3, the unguarded electrode.

The resistance of the specimen is given by the ratio of the applied voltage to the current measured. Here, the applied voltage was kept constant at 480 volts and the time of electrification was one minute. Current was measured several times in this way. Three samples (filter paper and two different micas)

---

(2) ASTM Standard Methods of Test for Electrical Resistance of Insulating materials.
(3) Power Supply: Heathkit Regulated Power Supply, Model PS-4
Ammeter : Keithley Multi-Range Electrometer, Model 610 B
Resistivity Adapter: Keithley Resistivity Adapter, Model 6105

were used in the experiments. The results of measurements are tabulated in Appendix III A.

From the geometry of the resistivity adapter and by the definition of resistivity, the volume resistivity can be calculated by using the relation;

$$\rho = \frac{A}{t} R \qquad (3.1)$$

where;

ρ = volume resistivity

A = the effective area of the guarded electrode for the particular electrode arrangement employed

t = the average thickness of the sample

R = resistance of the specimen

The effective area A for the particular electrode arrangement is given by:

$$A = \frac{\pi}{4} (D_1 + Bg)^2 \quad \text{sqcm.} \qquad (3.2)$$

where

g = gap width between the guarded and guard electrodes (Fig 3.2b)

B = a fraction related to the g/t.(4)

The correction factor Bg is introduced due to the effect of fringing of the electrical fields at the edges of the guarded electrode. Fringing occurs if the specimen material is homogeneous and isotropic. In this case, since we are dealing with thin films of specimen,(of a thickness of 10^{-3} cm.) it is acceptable to adopt a correction given by Bg = 0.883t. (5) Then the

---

(4) ASTM Designation D 257-61, Appendix I, pp. 131, 132
(5) Ibid.

effective area becomes:

$$A = \frac{\pi}{4} (D_1 + 0.883\, t)^2 \text{ sqcm.} \qquad (3.3)$$

Volume resistivities of the three samples have been calculated by using (3.1) and the results are included in Appendix III A. The results agree with the usual values of resistivity found in the Standard Handbook for Electrical Engineers by A.E. Knowlton, which states that for mica ".. the volume resistivity is of the order of 10^{12} to 10^{15} ohm.cm."

The ambiguity in the order of these values stems from the fact that resistivities of materials tested depend on humidity and temperature. Resistivity decreases with increasing temperature and humidity. This is more true for surface resistivity; and at relatively high levels of humidity (higher than 25%) most of the current leaks on the surface film if the volume resistance is more than 10^{14} ohms, and it becomes impossible to measure the volume resistivity without using special electrode arrangements as was done in this case by using a guard electrode.

It should also be noted here that it was this fact that led us to suspect whether the currents flowed through the surface or the volume of the dielectric in the case of the Electro-odocell.

The table on the next page shows the variation of surface resistivity with humidity for a few materials.

S u r f a c e R e s i s t i v i t y : As has already been mentioned, the surface resistivity of a material is important

under certain humidity conditions and may be misleading if not considered. In our experiments, surface resistivities of the

Material	Surface Resistivity (ohms)			Volume Resisitivity (ohm.cm)
	50%	70%	90%	
Mica	$2x10^{10}$	$4x10^{8}$	$8x10^{6}$	$2x10^{14}$
Porcelain	$6x10^{8}$	$7x10^{6}$	$5x10^{4}$	$3x10^{11}$
Quartz	$3x10^{9}$	$2x10^{6}$	$2x10^{5}$	$5x10^{15}$

Table 3.I (6) Resistivities of Solid Dielectrics

three samples already mentioned were also determined by using the same electrode arrangement as in the case of volume resistivity measurements with, however a different circuit connection. Fig 3.3 shows the circuit diagram.

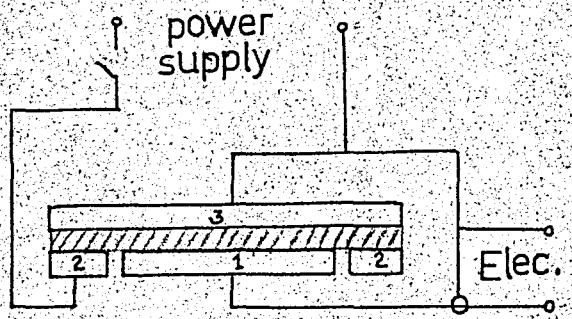

Fig 3.3

Here also the same arguments concerning the electrode dimensions of the equipment and the effects of finging apply, as in the case of volume resistivity measurements.

By the use of the above circuit, surface resistivity can be calculated from:

$$\sigma = \frac{P}{g} R \text{ ohms} \qquad (3.4)$$

where;

σ = surface resistivity in ohms

(6) Taken from Standard Handbook for Electrical Engineers A.E. Knowlton, Mc Graw Hill Book Comp., p. 4-366

g = the gap width between the guarded and the guard electrodes (Fig 3.2b)

P = the effective perimeter of the guarded electrode for the particular electrode arrangement

R = resistance of the specimen

Here P is given by:

$$P = \frac{2\pi g}{\ln D_2/D_1} \qquad (3.5)$$

but since g is small the approximate relation;

$$P = \pi D_o$$

will suffice for all practical purposes, (7) where, $D_o=(D_1+ D_2)/2$

Relation (3.5) for the guarded electrode perimeter takes into account the fringing at the edges. It should also be noted here that very little is known about the variation of surface resistivity with potential gradient or current density, but there is some evidence that such variations are significant.

Surface resistivities of the three samples were calculated on the basis of the above facts and the results found were consistent with the values in handbooks. The results of surface resistivity measurements are given in detail in Appendix III A.

VOLUME RESISTANCE OF THE DETECTOR DIELECTRIC:

Having determined the resistivities of the dielectrics, the resistance of a specific sample having a certain geometry can be calculated by using the relation given by (3.1). Fig 3.4 illustrates the electrode arrangement of the Electrodocell (ECC).

---

(7) ASTM Designation D 257-61 Appendix II, p. 133

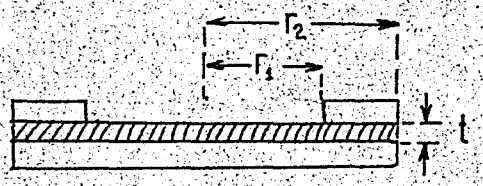

Fig 3.4

The ground electrode is a ring of inner radius r_1 and outer radius r_2. The inner high potential electrode is a disk of radius r_2. The dielectric fills the space between a metal ring and a metal disk and therefore the volume resistance in a direction perpendicular to the electrodes will be given by:

$$R = \rho \frac{t}{A} \qquad (3.6)$$

where A is given by:

$$A = \pi (r_2^2 - r_1^2) \qquad (3.7)$$

and (3.6) becomes

$$R = \rho \frac{t}{\pi (r_2^2 - r_1^2)} \qquad (3.8)$$

Here, it has been assumed that the current will flow along the shortest path from one electrode to the other and that the portion of the dielectric coinciding with the hole of the ring-shaped electrode will not contribute appreciably to its resistance.

The effect of considering the neglected portion would have lowered the resistance; but for our purposes it is appropriate to adopt the above assumption. The values of volume resistance calculated from (3.8) are given in Appendix III A.

The second approach to the determination of the volume resistance was the direct method, in which the detector was subjected to voltages up to 450 volts and the current passing through the transducer was measured by an ammeter. Fig 3.5 shows

the circuit diagram for this second method.

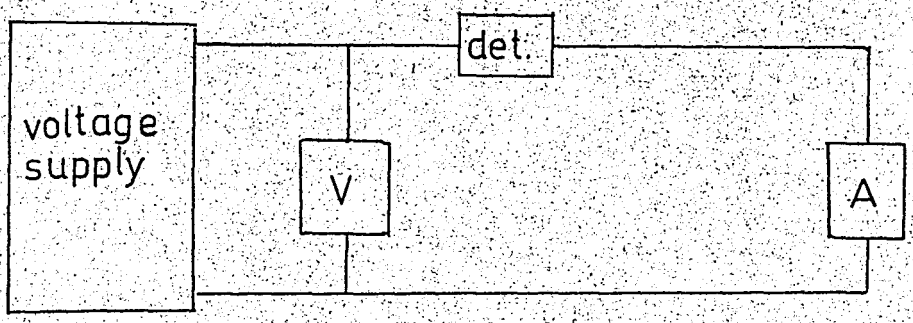

Fig. 3.5

It should be noted here that in this method, one is measuring not only the volume resistance of the dielectric but also the surface resistance and the cable leakage resistance. (8)

However, for reasons that will become evident later in this chapter, it will be only stated here that the resistance measured by this method is in fact the volume resistance of the dielectric alone.

The results of experiments performed with this circuit using mica and paper are given in Appendix III C, as the Graphs I to V.

An important result obtained from these experiments was that the EOC was a bilateral element. That is, its resistance was identical from both directions.

A third approach to the determination of the dielectric resistance will be mentioned later in this chapter in connection with capacitance measurements.

SURFACE RESISTANCE:

On the basis of the calculated surface resistivity, the sur-

(8) Cable leakage resistance is so high that it will be neglected as it is parallel with the dielectric resistance.

face resistance can be approximated as follows.

The surface resistance of a material is directly proportional to its length and inversely proportional to its width. The surface to be considered here can be approximated by the area of a rectangle whose longer dimension is given by $\pi D/4$ and its shorter dimension by D/2. Then the total resistance of this surface from the center to the radius will be :

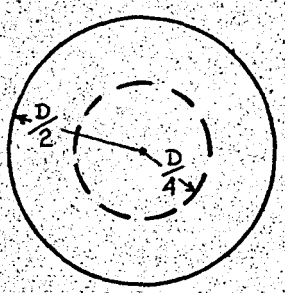

Fig. 3.6

$$R_s = \frac{\text{length}}{\text{width}} = \sigma \frac{D/2}{2\pi\, D/4} = \frac{\sigma}{\pi} \qquad (3\text{-}9)$$

The results of surface resistance calculated by this method are given in Appendix III C.

Finally the total resistance of the dielectric was calculated as the parallel combination of the volume and surface resistances. These results are found also in Appendix III C.

At this point we refer to a previous statement that the result of the direct measurements of the transducer resistance did in fact give the volume resistance. This is because there is no such resistance as surface resistance offered by the dielectric for the given electrode arrangement. When different rings of hole area were inserted into the open surface of the dielectric, which would mean the short-circuiting (or reducing) of the surface, there were no changes in the resistance measured, although appreciable change occured in the capacitance of the transducer.

From here on, therefore, we will not speak of the surface resistance of the dielectric, but only of a single resistance: its

volume or total resistance.

Before going to another section, it will be convenient here to summarize and add a few comments about the results of the experiments mentioned in this part.

C o n c l u s i o n s :

1. As can be seen from the tables and curves in Appendix III, the calculated values and measured values of resistance do not agree with each other, the calculated value being at least one hundred times larger. (For example, for dotted mica R (calculated) = 10^{11} ohms. R (measured) = 10^{9} ohms.)
2. Direct measurement of resistance by using the Model 610 B Electrometer in Ohmmeter operation does not give convincing results due to interference from external effects, i.e. voltages induced in the cable leads of the instrument.
3. Resistance is bilateral.
4. Pressure on the dielectric changes the transducer resistance.
5. Resistance changes with humidity. It decreases as humidity is increased. This is more pronounced with paper although small changes are observed with mica.
6. Surface reducing rings do not have any effect on the resistance, therefore there is almost no leakage current on the surface of the dielectric.

In the next section, an additional experiment with the Cathode Ray Oscilloscope will show that the value of resistance as found by the Voltmeter Ammeter Method (Direct Method) is more correct.

3.3 DIELECTRIC CAPACITANCE

The second element of importance in the transducer is its capacitance. The capacitance of the transducer (consisting of the dielectric capacitance, capacitance of the leads and metal housing) was measured first by an A.C. bridge (9) and then by the help of a circuit including a cathode ray oscilloscope.

Bridge Measurements

Capacitance was measured again with three samples of dielectric as in the case of resistance measurements. Furthermore, four cap areas were used to show the effect of area on capacitance.

The Bridge indicates the capacitance of the unknown branch when it is balanced at the proper values of C and D of the capacitive branch.

Here C is read either as C_s, the capacitance of a series connection as shown in Fig. 3.7a, or as C_p, the capacitance of a parallel connection as in Fig. 3.7b.

Fig. 3.7a

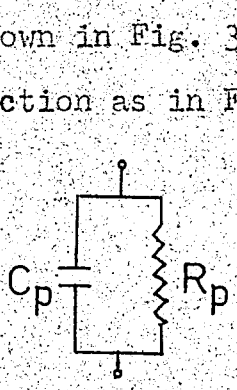

Fig. 3.7b

Whether the bridge will come to balance at ranges of C_s or C_p depends upon the order of the resistance associated with the capacitance. When balance is obtained at ranges of C_s, as in our case, the equivalent parallel combination components are given by,

---

(9) Type 1650-A Impedance Bridge, General Radio Company.

$$C_p = \frac{1}{1 + D^2} C_s \qquad \text{and} \qquad R_p = \frac{1}{\omega C_p D} \qquad (3\text{-}9)$$

where D is called the dissipation factor of the capacitance.

As can be seen from the second of relations (3-9) the dielectric resistance would be calculated, had it been possible to record an exact value of D. In fact, values of R calculated in this way gave much lower values of resistance, which simply meant that such low values would be enough to bring the capacitive element into balance.

In the experiments, it was seen that the values of D were very small compared to unity in all cases, which meant that C_s and C_p were approximately equal to each other.

A series of experiments were made to see the effect of dielectric material and cap area; in all of these experiments the same detector was used. Other experiments were also conducted with different detectors, which had their own characteristic capacitances. The results of the former are given in Appendix III B.

A series of bridge measurements was also made to see the effect of thickness of the dielectric. The results of the data from these experiments were plotted as thickness vs. capacitance. (See Appendix III C, Graphs VII and VIII.) It can be seen from these graphs that an approximate linear relationship exists between thickness and capacitance. That is,

$$C = k \frac{S}{t} \qquad (3\text{-}10)$$

This is so because the plate dimensions are at least a hundred times larger than the thickness of the dielectric; therefore, the capacitor can be considered as having infinite plate area, and an approximately linear relation holds. The effect of plate area was also investigated and it was found that capacitance increased with increasing plate area. See Appendix III B, Tables B2 and B3.

An Experiment with the Cathode Ray Oscilloscope: (CRO)

This experiment served to determind both the resistance and capacitance. The block diagram of the circuit used is shown in Fig. 3.8.

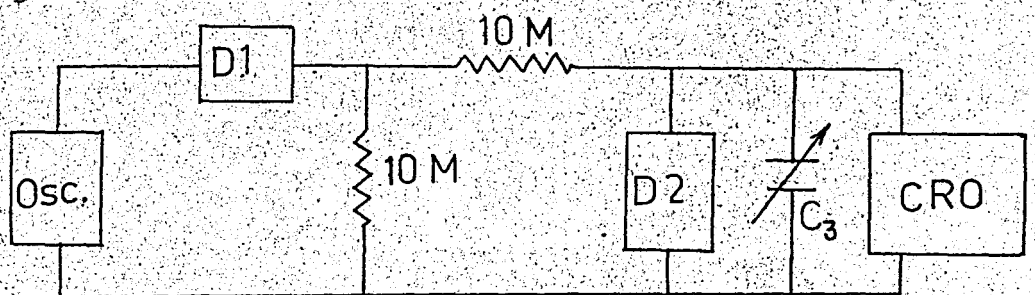

Fig. 3.8

The electrical circuit is as given in Fig. 3.9.

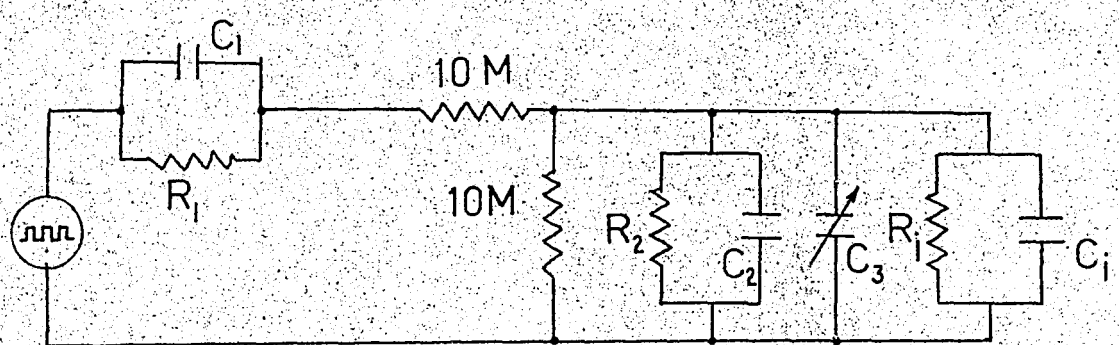

Fig. 3.9

For this circuit the following analysis can be made. The input is a square wave of appropriate frequency. When the wave shape on the CRO becomes independent of frequency the circuit is said to satisfy the relations:

$$R_1C_1 = RC \qquad \text{and} \qquad e_2 = e_1 \frac{R}{R_1 + R} \tag{3-11}$$

where $C = C_2 + C_i + C_3$ and $R = \frac{R_2R_i}{R_2 + R_i}$

Here, since R_2 is very high, and R_i = 1 M , the input resistance of the CRO, then $R \cong$ 1 M . The cathode ray oscilloscope has an input capacitance (C_i) of 47 p F.

Now, when the frequency is small, attenuation through the circuit is caused mainly by the resistive elements; therefore, independence from frequency can be assured by observing no changes in the amplitude of the output voltage.

The following data were obtained.

Input voltage at all frequencies: 24 volts.

f	Output Voltage	C_3 setting
5000	16.2 mV.	1 μ F
500	10.0 mV.	1.5 μ F
50	5.0 mV.	3 μ F

Now since $C_3 >> C_2 + C_i$; $C \cong C_3$

From (3-11):

$$\frac{e_2}{e_1} = \frac{R}{R_1 + R} = \frac{R}{R_1} \tag{3-12}$$

(note that $R \ll R_1$)

$$R_1 = R \frac{e_1}{e_2} \qquad (3\text{-}13)$$

at $e_2 = 10$ mV.

$$R_1 = \frac{1M \times 24}{10 \times 10^{-3}} = 2.4 \times 10^9 \text{ ohms.}$$

This verifies the correctness of the order of capacitance and resistance of the transducer as found in the measurements of the previous sections.

Alternately using the relation $R_1C_1 = RC$ with $C_3 = 1.5\,\mu F$. $C_1 = 220$ pF (from the bridge measurements)

$$R_1 = \frac{C}{C_1} R = \frac{1.5 \times 10^6 \text{nF}}{220\text{pF}} 1M \cong 10^9 \text{ ohms,}$$

which shows again that $R_1 \cong 10^9$ ohms and $C_1 = 220$ pF.

It should be noted here that the circuit of Fig. 3.10 used in the above experiment was deliberately chosen so as to give responses similar to the ones obtained from the Electro-Odocell, when a square wave input was applied to its input terminals. The use of a second detector as a circuit element was necessary to have a match with the resistance and capacitance of the first detector.

A final experiment using another circuit arrangement with one detector consisted of finding the half power point of the detector impedance and thus checking the correctness of the capacitance value. The circuit diagram is illustrated in Fig. 3.10.

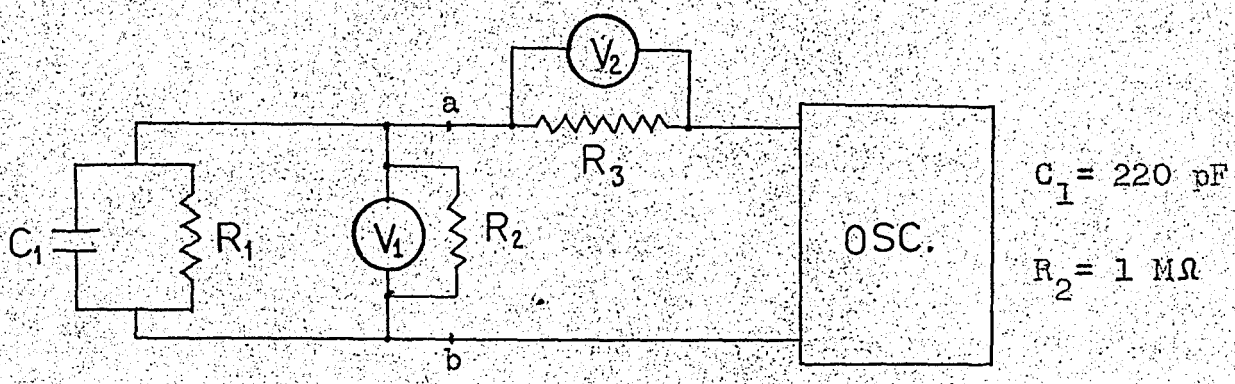

Fig. 3.10

Here voltmeter V_1 has an internal resistance R_2 and is in parallel with the detector resistance R_1. The circuit is supplied from an oscillator and the current drawn by the impedance to the left of points a, b is calculated as the drop across a known resistance R_3. The voltage V_1 derived by this current gives the impedance Z_{ab} at several frequencies of the input. When this impedance is plotted against frequency, there will be one frequency where;

$$w = \frac{1}{RC} \qquad (3\text{-}14)$$

which is called the half power frequency. The corresponding impedance then will be

$$|Z_{ab}| = \frac{R}{2} \qquad (3\text{-}15)$$

the half power impedance. See Appendix III C, Graph VI.

These relations are obtained by the following analysis;

From the circuit

$$Z_{ab} = \frac{R/\frac{1}{jwc}}{R + 1/jwc} = \frac{R}{1 + jwRC} \qquad (3\text{-}16)$$

where;

$$R = \frac{R_1 R_2}{R_1 + R_2} \cong R_2 \quad (\text{since } R_1 \gg R_2) \qquad (3\text{-}16)$$

Therefore, at $w = 0$, $Z_{ab} = R \cong R_2 = 1\ M\Omega$.

By interpolation from the Z_{ab} v.s. f curve (Graph VI in Appendix III C), this value is found to be 1.25 $M\Omega$, which is agreeable with the actual value 1 $M\Omega$. At the half power impedance:

$$|Z_{ab}| = \frac{R}{\sqrt{2}} = \frac{1.25}{\sqrt{2}} = 0.885\ M\Omega$$

This value of impedance corresponds to f = 830 cps.

Now since,

$$R = \frac{1}{WC} \quad \text{(at the half power point)}$$

R can be calculated theoretically from,

$$R = \frac{1}{(6.28)(830)(2.20 \times 10^{-10})} = 0.875\ M\Omega .$$

Therefore the value of $C_1 = 220$ pF used in finding R from the half power relation was correct, since it gave a value very nearly equal to the experimental value; 0.885 $M\Omega$.

C o n c l u s i o n s :

1. Capacitance increases with increasing effective dielectric area and decreasing dielectric thickness.

2. Capacitance increases with increased pressure on the dielectric.

3. In the case of mica as the detecting dielectric, the main variable for a given odorant seems to be the capacitance. The responses of the circuit in Fig. 3.9, to varying water vapor at the transducer dielectric were as follows on the oscilloscope:

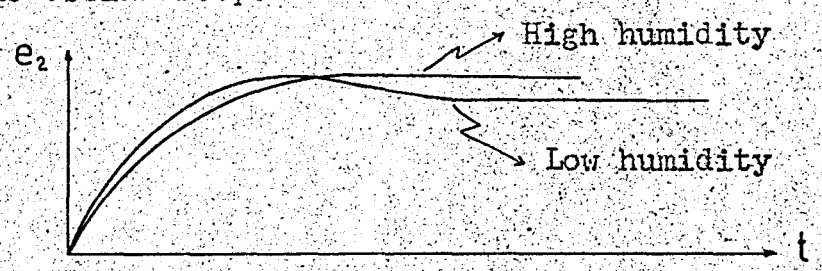

Fig. 3.11

Fig. 3.11 implies decreases in both R_1 and C_1 in the circuit of Fig. 3.10, when water vapor is increased, the effect being more pronounced on C_1.

CHAPTER IV

APPROACHES TO THE ELECTRICAL EQUIVALENT CIRCUIT:

4.1 RESPONSE CHARACTERISTICS:

As has been mentioned previously in Chapter 2, the responses obtained in measurements with several odorants had the general forms illustrated here again by Figures 4.1a and 4.1b. See also Appendix II for acetone response.

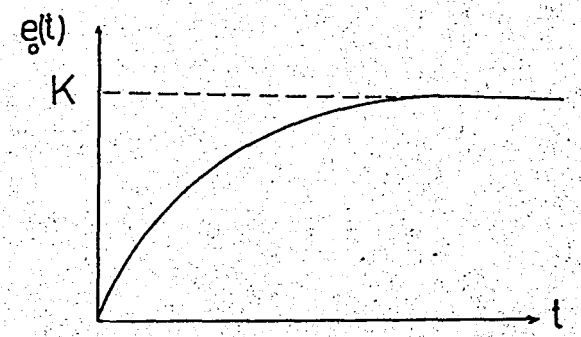

Fig. 4.1a

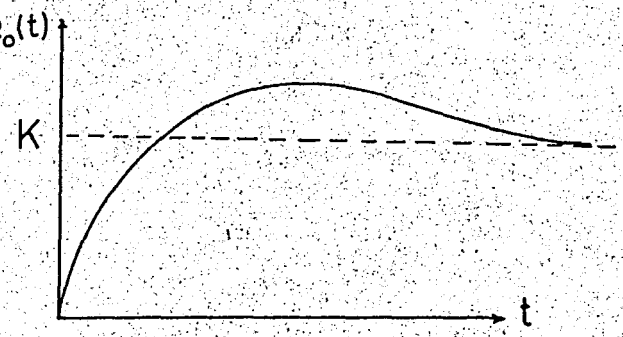

Fig. 4.1b

To have any of these output characteristics from an input function - transfer function pair, there is no unique solution. That is, a number of such different pairs can produce the same output.

However, if we restrict ourselves to a certain network of a known transfer function, as for example the one represented by Fig. 4.3, there will be only a few choices (which can be related to each other in some way) for the input function, to have the desired output.

In this chapter, the mathematical analysis leading to an input function which will give that desired output will be considered.

4.2 EFFORTS TOWARDS AN ELECTRICAL EQUIVALENT CIRCUIT

Based upon the data obtained from the measurements by the EOC, an electrical model, which would give the same response for a given input was considered as the first approach to the following analysis.

Here, the main idea was to set up an electrical analog characterized by lumped constants. A rough representation as implied by the physical conditions of the transducer as it is connected to a measuring instrument, is shown by Fig. 4.2 below.

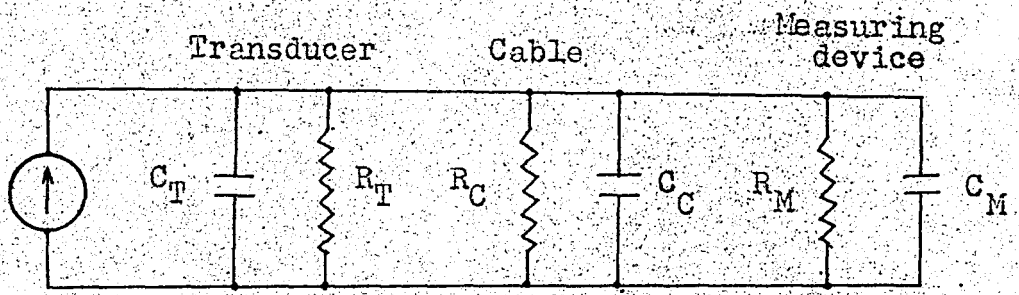

Fig. 4.2

The underlying assumption carried by this representation is that there is a charge rate of change on the transducer dielectric, produced by the molecules collecting on the dielectric surface. This buildup of charge is represented by a current generator, between the two plates of an equivalent capacitance of the dielectric.

The portion of the equivalent circuit, representing the transducer in Fig. 4.2 takes into account also the resistance of the insulator dielectric and the capacitance of the metal housing.

Next we consider the capacitance and the leakage resistance of the cable as connected in parallel with the transducer circuit. Finally there is the input capacitance and resistance of the measuring instrument, also in parallel with the preceding two sections.

In the analysis that follows, however, we do not speak of the cable resistance and capacitance alone, but incorporate them in the transducer constants, since in the measurements of these elements, the transducer and the cable were never separated from each other.

Based on the preceding discussion, the circuit of Fig. 4.2 can be reduced to the one shown in Fig. 4.3, with newly defined constants.

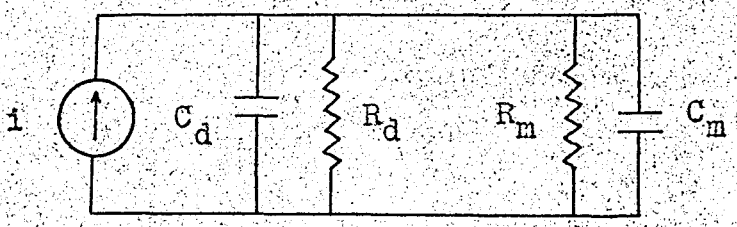

$$C_d = C_T + C_C$$

$$R_d = \frac{R_T R_C}{R_T + R_C}$$

Fig. 4.3

This circuit can also be represented by a new arrangement of the network elements, in which the current generator is replaced by its equivalent voltage generator. This will be done in the next section where we discuss the input functions. We assume the circuit of Fig. 4.3 to be the electrical equivalent circuit of the Electro-Odocell and start our analysis for the input phenomenon.

4.3 TRANSFER FUNCTION OF THE EQUIVALENT CIRCUIT

In the analysis of the input functions which will give the desired output responses, it will be convenient first to convert the current generator of Fig. 4.3 to a voltage generator as in Fig. 4.4 and change the subscripts so as to have more conveniently $C_d = C_1$, $R_d = R_1$, $R_m = R_2$, $C_m = C_2$.

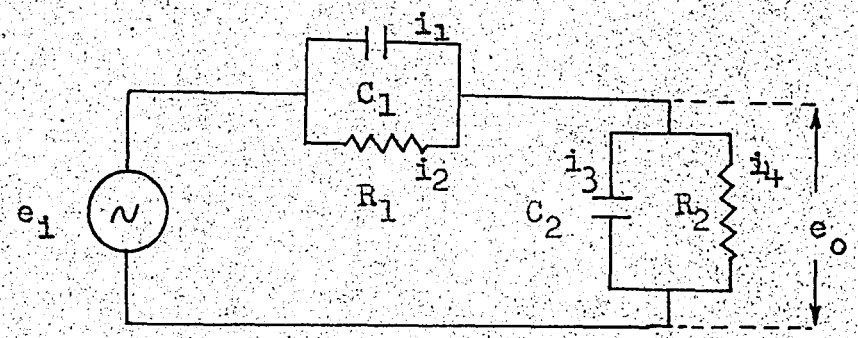

Fig. 4.4

The transfer function of the assumed circuit for a voltage input can be derived by refering to Fig. 4.5.

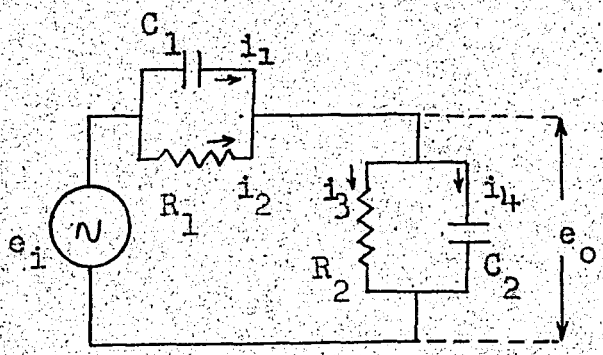

Fig. 4.5

$$e_i = i_2 R_1 + i_3 R_2 \qquad (4.1)$$

$$\frac{1}{C_1}\int i_1 \, dt = i_2 R_1 \qquad (4.2)$$

$$\frac{1}{C_2}\int i_4 \, dt = i_3 R_2 \qquad (4.3)$$

$$i_2 + i_1 = i_3 + i_4 \qquad (4.4)$$

From (4.4)

$$i_4 = i_1 + i_2 - i_3 \qquad (4.5)$$

From (4.2)

$$\frac{1}{C_1} i_1 = R_1 \frac{di_2}{dt} \quad , \text{therefore} \quad i_1 = R_1 C_1 \frac{di_2}{dt} \tag{4.6}$$

From (4.1)

$$i_2 = \frac{ei - i_3 R_2}{R_1} \quad \text{and} \quad \frac{di_2}{dt} = \frac{1}{R_1}\left(\frac{de_i}{dt} - R_2 \frac{di_3}{dt}\right) \tag{4.7}$$

Combining (4.6) and (4.7),

$$i_1 = R_1 C_1 \left[\frac{1}{R_1}\left(\frac{de_i}{dt} - R_2 \frac{di_3}{dt}\right)\right] \tag{4.8}$$

From (4.3),

$$\frac{1}{C_2} i_4 = R_2 \frac{di_3}{dt} \quad \text{and} \quad i_4 = R_2 C_2 \frac{di_3}{dt} \tag{4.9}$$

Substituting (4.7) and (4.8) in (4.5),

$$R_2 C_2 \frac{di_3}{dt} = R_1 C_1 \left[\frac{1}{R_1}\left(\frac{de_3}{dt} - R_2 \frac{di_3}{dt}\right)\right] + \frac{1}{R_1}(e_i - i_3 R_2) - i_3 \tag{4.10}$$

Collecting the like terms:

$$\frac{di_3}{dt}(R_2 C_2 + R_2 C_1) + i_3\left(\frac{R_2}{R_1} + 1\right) = \frac{1}{R_1} e_i + C_1 \frac{de_i}{dt} \tag{4.11}$$

Taking the Laplace transform of (4.11), and imposing the initial conditions;

$$i_3(0+) = 0 \quad ; \quad e_i(0+) = 0 \quad \text{we obtain}$$

$$I_3(s)\left[s(R_2 C_2 + R_2 C_1) + \left(\frac{R_2}{R_1} + 1\right)\right] = E_i(s)\left(\frac{1}{R_1} + sC_1\right) \tag{4.12}$$

$$I_3(s) = \frac{E_i(s)\left(\frac{1}{R_1} + sC_1\right)}{\left(\frac{R_2}{R_1} + 1\right) + s(R_2C_2 + R_2C_1)} = \frac{E_i(s)(1+sR_1C_1)}{R_1+R_2+ sR_1R_2(C_1+C_2)} \qquad (4.13)$$

Now, $E_o(s) = R_2 I_3(s)$ (4.14)

$$E_o(s) = \frac{E_i(s)\, R_2(1 + sR_1C_1)}{R_1 + R_2 + sR_1R_2(C_1 + C_2)} \qquad (4.15)$$

$$\frac{E_o(s)}{E_i(s)} = \frac{R_2(1 + sR_1R_2)}{(R_1 + R_2) + sR_1R_2(C_1 + C_2)} \qquad (4.16)$$

(4.16) is the transfer function of the assumed equivalent circuit.

At this point we shall introduce the substitutions,

$$K = \frac{C_1}{C_1 + C_2} \quad ; \quad a = \frac{1}{R_1C_1} \quad ; \quad b = \frac{R_1 + R_2}{R_1R_2(C_1 + C_2)} \qquad (4.17)$$

Then the transfer function becomes:

$$H(s) = \frac{E_o(s)}{E_i(s)} = K\frac{(s + a)}{(s + b)} \qquad (4.18)$$

Similarly, for a current input, the transfer impedance $Z(s)$ can be found to be:

$$Z(s) = \frac{1}{(C_1 + C_2)} \cdot \frac{1}{(s + b)} \qquad (4.18a)$$

where:

$$b = \frac{R_1 + R_2}{R_1R_2(C_1 + C_2)}$$

4.4 VOLTAGE INPUT FUNCTIONS:

A. Response to a step function:

Let us consider a step function given by $e_i = E_i\, u(t)$ having the Laplace transform; $E_i(s) = \frac{E_i}{s}$.

From (4.18):

$$E_o(s) = E_i(s)\, H(s) = \frac{E_i\, K\,(s + a)}{s(s + b)} \qquad (4.19)$$

By the method of partial fractions (or the Residue Theorem),

$$e_o(t) = E_i\, K\left[\frac{a}{b} + \left(1 - \frac{a}{b}\right) e^{-bt}\right] \qquad (4.20)$$

where the constants a , b and K are as defined previously, by (4.17). When this response is plotted, we have the curve in Fig. 4.6.

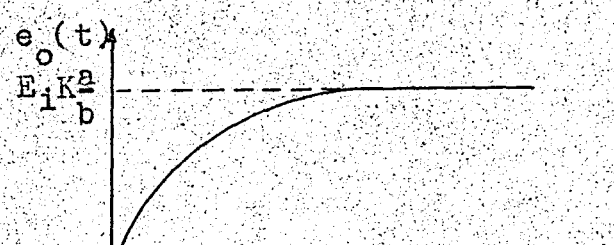

Fig. 4.6

This curve implies that a step function input may be an answer to our question as it provides a response similar to the ones obtained from the experiments. This does not mean that the molecules are collected on the dielectric surface instantaneously, because the actual physical phenomenon is the generation of current, whose expression in time domain is given by the inverse transform of,

$$\left[\frac{E_i(s)}{Z_1(s)}\right] \qquad \text{that is,}$$

$$i_i(t) = \frac{dq}{dt} = \mathcal{L}^{-1}\left[\frac{E_i(s)}{Z_1(s)}\right] \qquad (4\text{-}21)$$

where $Z_1(s)$ is the transform impedance of R_1 and C_1 in parallel.

This point will be taken up again later in this chapter, in connection with other input functions.

B. Response to a linear input:

In this case the input function is given by $e_i = E_i t$ and its Laplace transform by $Ei(s) = \frac{Ei}{S^2}$.

From (4.18),

$$E_o(s) = E_i(s)\, H(s) = \frac{E_i}{s^2} \cdot \frac{K(s+a)}{(s+b)} \qquad (4.22)$$

Again by the method of partial fractions (or the Residue Theorem),

$$e_o(t) = E_i K \left[\frac{b-a}{b^2} - \frac{b-a}{b^2} e^{-bt} + \frac{a}{b} t \right] \qquad (4.23)$$

When this expression is plotted we obtain the curve in Fig. 4.7.

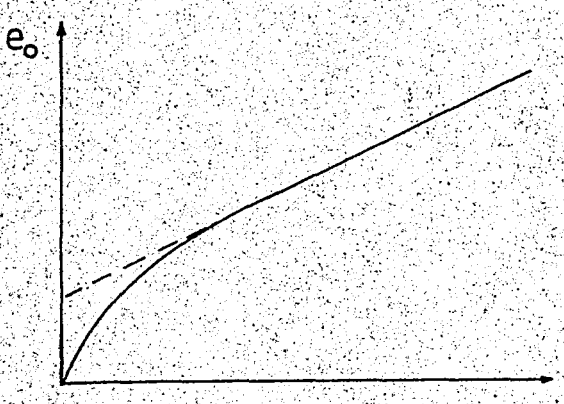

Fig. 4.7

This response implies that the assumed input cannot be of the form

$$e_i = KE_i t$$

because as $t \to \infty$, the output also tends to go to infinity, which is not the case with the experiments carried out with odorants for several hours. Therefore, the charge build-up leading to linear input in the equivalent circuit seems to be out of question.

C. Response to exponential rise:

The input function assumed here is given by

$$e_i = E_i(1 - e^{-\alpha t}) \qquad (4\text{-}24)$$

whose Laplace transform is,

$$E_i(s) = \frac{E_i \alpha}{s(s + \alpha)} \qquad (4\text{-}24a)$$

From (4-18) for such an input

$$E_o(s) = E_i(s)\, H(s) = \frac{E_i \alpha}{s(s + \alpha)} K \frac{(s + a)}{(s + b)} \qquad (4\text{-}25)$$

From the Residue Theorem:

$$e_o(t) = E_i K \left[\frac{a}{b} + \frac{\alpha(a - b)}{b(b - \alpha)} e^{-bt} + \frac{(\alpha - a)}{(b - \alpha)} e^{-\alpha t} \right] \qquad (4\text{-}26)$$

In these expressions, the constant α is related to the input function and, therefore, to the properties of the specific odorant. As is shown by (4-26), output response depends on this constant α and the constants a, b and K of the assumed network. Graphs I to III in Appendix IV illustrate the forms of (4-26) for a few cases of α, a and b relationships.

All possible cases of how α may be related to a and b are listed in Table 4.I.

Table 4.I

$a > b$	$b > a$
1. $a > b > \alpha$	6. $\alpha > b > a$
2. $a > \alpha > b$	7. $b > a > \alpha$
3. $\alpha > a > b$	8. $b > \alpha > a$
4. $a > b = \alpha$	9. $b > a = \alpha$
5. $\alpha = a > b$	10. $b = \alpha > a$
11. $a = b > \alpha$	
12. $\alpha > a = b$	
13. $a = b = \alpha$	

All these relationships result in one or the other of the desired output functions mentioned earlier in this chapter. There are three cases, (6., 8., 10.), namely $\alpha > b > a$, $b > \alpha > a$ and $b = \alpha > a$ which would give an output function like that of Fig. 4.1b; all the remaining cases resulting in output functions like that of Fig.1a. This can be understood by a quick glance at the relation giving the time of maximum output in (4.27) which is found by setting the derivative of (4.26) equal to zero.

$$t = \frac{1}{b - \alpha} \ln \frac{(b - a)}{(\alpha - a)} \qquad (4.27)$$

This equation provides a positive t, only for the above three cases, 6., 8., and 10.

Responses obtained by acetone had the form of Fig. 4.1b,

and, therefore, the cases of α , b , a relationships giving such a response should be considered for acetone.

In Appendix IV, Graphs I, II and III represent the plots of equation (4.26) with values of a , b , and α as calculated from the results of measurements in Chapter III.

These plots have the following equations.

Assuming $E_1 = 1mV$ $R_2 = 10^{14}$ohms $R_1 = 10^9$ohms

$C_2 = 22pF$ $C_1 = 220pF$

$$a = \frac{1}{R_1 C_1} = 4.55 \qquad b = 4.14 \qquad K = \frac{C_1}{C_1 + C_2} = 0.91$$

Graph I, $b < a < \alpha$ (with $\alpha = 5$ assumed)

$$e_o(t) = 1 - 0.525\, e^{-4.14t} - 0.476\, e^{-5t} \qquad (4.28)$$

Graph II, $b < \alpha < a$ (with $\alpha = 4.3$ assumed)

$$e_o(t) = 1 - 2.42\, e^{-4.14t} + 1.42\, e^{-4.3t} \qquad (4.29)$$

Graph III, $\alpha < b < a$ (with $\alpha = 3$ assumed)

$$e_o(t) = 1 + 0.238\, e^{-4.14t} - 1.238\, e^{-3t} \qquad (4.30)$$

As can be seen from these plots, none of the above equations give the desired response for acetone. Furthermore, the time scale has to be chosen very small compared to the actual experimental curves due to the fact that the values of a , b , and α are large (i.e. time constants are very small).

To adapt equation (4.26) for the experimental results of acetone response, one of the cases (6., 8., or 10.) must hold.

Group IV in Appendix IV represents a close approximation to the actual acetone response. The constants of the equation represented by that graph were determined by trial and error, making use of the linear portions of the experimental curve.

The output equation represented by Graph IV has the expression,

$$e_o(t) = 40.6\left[0.5 - 0.782\, e^{-0.1t} + 0.282\, e^{-0.061t}\right] \qquad (4.31)$$

with $a = 0.05$, $b = 0.1$ and $\alpha = 0.061$.

A more accurate representation of the acetone response was found by the following analysis.

Starting from Equation (4-26) and defining:

$$\frac{a}{b} = A \;;\; B = \frac{\alpha}{b} \;;\; K_2 = \frac{K_1}{1-B} \quad \text{and} \quad K_1 = E_i K \qquad (4.32)$$

we obtain the equation,

$$e_o(t) = K_2\left[A(1 - B) + B(A - 1)e^{-bt} + (B - A)e^{-Bbt}\right] \qquad (4.33)$$

and its derivative

$$e_o'(t) = K_2\left[-Bb(A - 1)e^{-bt} - Bb(B - A)e^{-Bbt}\right] \qquad (4.34)$$

Multiplying (4.33) by bB and adding (4.34) to it we obtain,

$$bBe_o(t) + e_o'(t) = K_2AbB(1 - B) + K_2Bb(1-A)(1-B)e^{-bt} \qquad (4.35)$$

Here a new set of constants is introduced where:

$$D = bB \;;\; C = K_2AbB(1-B) \;;\; F = K_2Bb(1-A)(1-B) \qquad (4.36)$$

and (4.35) takes the form

$$De_o(t) + e_o'(t) = C + F\, e^{-bt} \qquad (4.37)$$

This equation is more simple to deal with and its four constants can be evaluated from a knowledge of $e_0(t)$ and $e_0'(t)$ at four points of the output response.

We attempted to use the following data taken from the acetone response illustrated in Appendix II, to evaluate the constants of (4.26):

(I)	$t = 0$ sec.	$e_0(t) = 0$ mV	$e_0'(t) = 3.46$ mV/sec.
(II)	$t = 4.8$ sec.	$e_0(t) = 11.5$ mV	$e_0'(t) = 2.30$ mV/sec.
(III)	$t = 20.8$ sec.	$e_0(t) = 24$ mV	$e_0'(t) = 0$ mV/sec.
(IV)	$t = \infty$	$e_0(t) = 20.3$ mV	$e_0'(t) = 0$ mV/sec.

When this data was inserted in (4.37) the constants a , b , and K came out to be complex numbers. This meant that (4.26) would never represent the acetone response exactly but could provide an approximate expression for it, with real constants.

The new set of values, slightly different from the actual values, did give a solution with real constants and this approximating function was determined as follows;

(Ia)	$t = 0$ sec.	$e_0(t) = 0$ mV	$e_0'(t) = 4$ mV/sec.
(IIa)	$t = 4.75$ sec.	$e_0(t) = 11.5$ mV	$e_0'(t) = 2.30$ mV/sec.
(IIIa)	$t = 22$ sec.	$e_0(t) = 24$ mV	$e_0'(t) = 0$ mV/sec.
(IVa)	$t = \infty$	$e_0(t) = 18$ mV	$e_0'(t) = 0$ mV/sec.

Using this data in (4.37) we have:

$$4. = C + F \tag{4.38}$$

$$11.5D + 2.30 = C + F\, e^{-4.75b} \tag{4.39}$$

$$24D + 0 = C + F\, e^{-22b} \tag{4.40}$$

$$18D + 0 = C \tag{4.41}$$

From (4.38 and 41)

$$D = \frac{1}{18}(4 - F) \tag{4.42}$$

From (4.39 and 40)

$$12.5D - 2.3 = F(e^{-22b} - e^{-4.75b}) \tag{4.43}$$

and therefore:

$$D = \frac{1}{12.5} F(e^{-22b} - e^{-4.75b}) + 2.30 \tag{4.44}$$

From (4.42 and 44)

$$F = \frac{0.48}{0.695 + e^{-22b} - e^{-4.75b}} \tag{4.45}$$

From (4.38, 40 and 42)

$$F = \frac{1.34}{(0.33 + e^{-22b}} \tag{4.46}$$

Finally, from the last two equations we have

$$0.77 + 0.86\, e^{-22b} - 1.34\, e^{-4.75b} = 0 \tag{4.47}$$

This is an equation with exponential terms and is difficult to solve readily for (b). However, if the order of (b) for which the function approaches zero, is known, the value of (b) which makes it zero can be found by trial and error or by using a computer to try a set of values in the predetermined range. A computer was used in this case and the value of (b) for which (4.47) was satisfied was found to be 0.078.

Once (b) is found, the other constants, C , D and F , can be evaluated, and from these constants one can find the constants α , a and K_1 by using the relations in (4.32).

When this was done the following values of the constants were obtained.

$$\begin{aligned} a &= 0.027 \\ b &= 0.078 \\ \alpha &= 0.076 \\ K_1 &= 52 \text{ mV} \end{aligned} \qquad (4.48)$$

These values satisfy the restriction: $b > \alpha > a$, as they should for the considered response.

Hence, Equation (4.26) becomes:

$$e_0(t) = 52 \quad 0.336 - 24.83e^{-0.08t} + 24.50e^{-0.075t} \qquad (4.49)$$

This equation represents the output response for acetone more accurately than does Equation (4.31) .

At this point we go back to the three possible relationships (cases 6., 8., and 10. in Table 4.I) of the constants a , b , and α for acetone response. In all these three cases b is larger than a . Furthermore, from the measurements of Chapter III it is certain at least that R_2 is larger than R_1 and the value of detector capacitance lies between 100 - 200 micro-microfarads. These restrictions, however, do not allow (b) to be larger than (a) . Therefore, it can be concluded that although (4.26) with its constants related as in any of the possible cases mentioned above can represent the actual acetone response, the relationships among the constants a , b , and

α, do not conform with the experimental facts. Thus for acetone the assumed input function leading to (4.26) can not be accepted, but a different voltage or current input function should be considered.

The next section is devoted to the investigation of a current input function which would satisfy both the response characteristics of acetone and the previously measured circuit constant requirements.

4.5 CURRENT INPUT FUNCTIONS:

To deal with current input functions it is more convenient to use the configuration of the original circuit given by Fig. 4.3, only with a change in subscripts, as in Fig. 4.8.

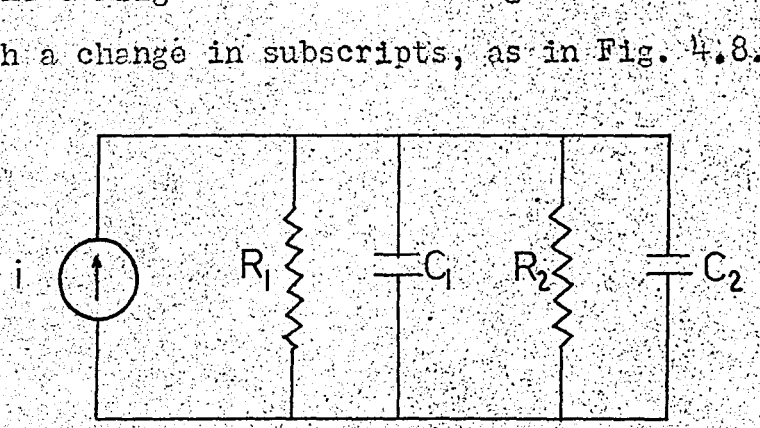

Fig. 4.8

Furthermore, to evaluate the constants of the charge generator equation readily, a charge expression will be considered, the time derivative of which yields the expression of the desired current generator.

A. Step current input:

$$q = Q_0 t \qquad i(t) = Q_0 \qquad I(s) = \frac{Q_0}{s} \tag{4.50}$$

With this current input the output will be:

$$e_o(t) = Z.i(t) \quad , \text{ or,} \tag{4.51}$$

$$e_o(t) = \mathcal{L}^{-1}\left[Z(s)\ I(s)\right] \tag{4.52}$$

From (4.18a), $Z(s) = \frac{1}{C_1 + C_2} \cdot \frac{1}{s + b}$, and

$$e_o(t) = \frac{Q_o R_1 R_2}{(R_1 + R_2)}\ (1 - e^{-bt}) \tag{4.53}$$

The plot of this function is given by Fig. 4.9. Such an input may be the answer for several odorants, but for acetone it can not be considered.

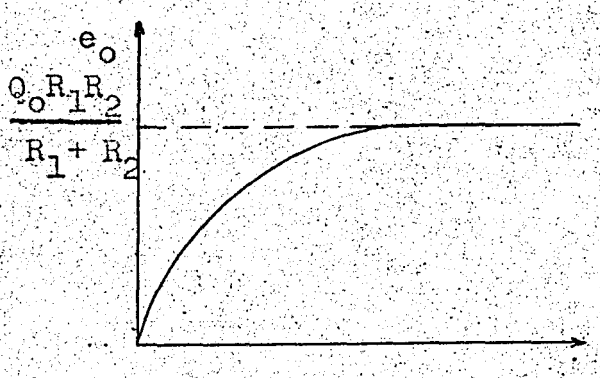

Fig. 4.9

B. Exponential current decay:

$$q = Q_o(1 - e^{-\alpha t})\ ;\ i(t) = Q_o \alpha e^{-\alpha t}\ ;\ I(s) = \frac{Q_o \alpha}{s + \alpha} \tag{4.54}$$

From (4.52)

$$e_o(t) = \frac{Q_o}{(C_1 + C_2)(b - \alpha)}\ (e^{-\alpha t} - e^{-bt}) \tag{4.55}$$

The graph of this equation is represented in Fig. 4.10.

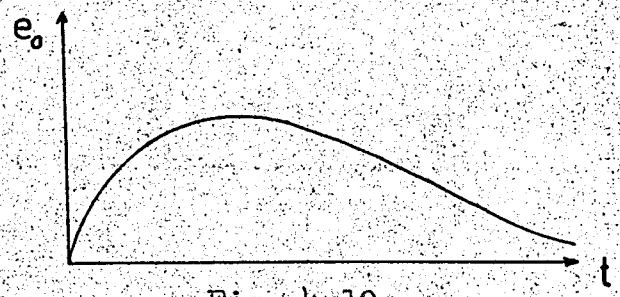

Fig. 4.10

Input can not be (4.54) either, because the output it produces does not resemble the acetone response.

Two other current input functions, neither of which give the desired output, are:

$$q = Q_0 + K(1 - e^{-\alpha t}) \qquad I(t) = K\alpha e^{-\alpha t} \tag{4.56}$$

$$q = Q_0 te^{-\alpha t} \qquad I(t) = Q_0 (1 - \alpha t) e^{-\alpha t} \tag{4.57}$$

C. Exponential current decay with a nonzero final value:

Here we consider the charge equation:

$$q = Kt - Q_0 e^{-\alpha t} \tag{4.58}$$

the time derivative of which produces the current generator function,

$$\frac{dq}{dt} = I(t) = K + Q_0 \alpha e^{-\alpha t} \tag{4.59}$$

and

$$I(s) = (K + Q_0 \alpha) \frac{s + r}{s(s + \alpha)} \tag{4.60}$$

where $r = \dfrac{K\alpha}{K + Q_0\alpha}$; or

$$I(s) = \frac{K\alpha}{r} \frac{s + r}{s(s + \alpha)} \tag{4.61}$$

From (4.52):

$$e_o(t) = \mathcal{L}^{-1}\left[\frac{K\alpha}{r(C_1+C_2)} \cdot \frac{(s+r)}{s(s+\alpha)(s+b)}\right] \qquad (4.62)$$

$$e_o(t) = \frac{K_1}{r}\left[\frac{r}{b} + \frac{\alpha(r-b)}{b(b-\alpha)}e^{-bt} + \frac{(\alpha-a)}{(b-\alpha)}e^{-\alpha t}\right] \qquad (4.63)$$

where $K_1 = \dfrac{K}{C_1 + C_2}$. When this function is plotted we obtain a curve similar to the acetone response, Fig. 4.11.

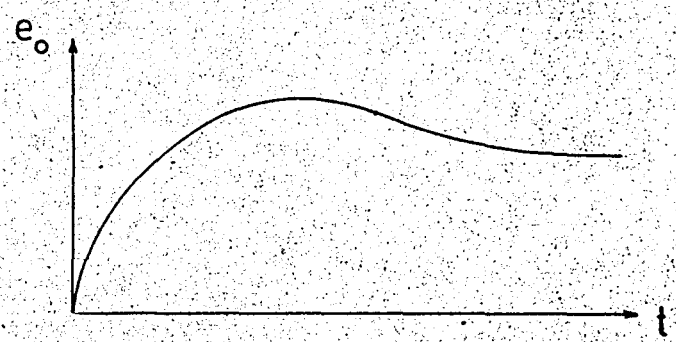

Fig. 4.11

Equation (4.62) has the same form as Equation (4.26), and, therefore, solutions of that equation can be assigned to (4.63), with a slight change in notation. Thus we obtain

$$\begin{aligned} b &= 0.078 \quad \text{sec.}^{-1} \\ \alpha &= 0.076 \quad \text{sec.}^{-1} \\ r &= 0.027 \quad \text{sec.}^{-1} \\ K_1 &= 1.4 \quad \text{mV/sec.} \end{aligned} \qquad (4.64)$$

From the above constants, K and Q_o can be found. If we take $C_1 = 200$ pF and $C_2 = 22$ pF,

$$K = K_1(C_1 + C_2) = 0.312 \times 10^{-12} \text{ Amperes}$$

$$Q_o = \frac{K(\alpha - r)}{r\alpha} = 7.45 \times 10^{-12} \text{ coul.}$$

When these constants are substituted in (4.63), we have,

$$e_o(t) = 52\left[0.336 - 24.8e^{-0.078t} + 24.5e^{-0.076t}\right] \text{ mV} \qquad (4.65)$$

It is seen that in this equation α and b are nearly equal. For the special case of $\alpha = b$, the determination of constants is greatly simplified and we obtain for this case,

$$\alpha = b = 0.090$$
$$r = 0.040 \qquad (4.66)$$

which when substituted in (4.67)

$$e_o(t) = \frac{K}{r(C_1 + C_2)}\left\{\frac{r}{b} - e^{-bt}\left[\frac{r}{b} - (b - r)t\right]\right\} \qquad (4.67)$$

yield the equation,

$$e_o(t) = 44.5\left[0.45 - (0.45 - 0.05t)\, e^{-0.09t}\right] \qquad (4.68)$$

which is the most accurate representation of acetone response in our experiments.

Graph V, in Appendix IV, gives a comparison of the representative equations derived in this section, for acetone.

4.6 INTERPRETATION OF THE INPUT FUNCTIONS:

I. Voltage Input Functions:

In Section 4.4, it was stated that the expression of the equivalent current input for a voltage input to the equivalent circuit is given by

$$i_i(t) = \mathcal{L}^{-1}\left[\frac{E_i(s)}{Z_1(s)}\right] \tag{4.69}$$

where $Z_1(s)$ is the transform impedance of R_1 and C_1 in parallel, equal to:

$$\frac{1}{C_1} \cdot \frac{1}{s+a} \qquad \text{where} \qquad a = \frac{1}{R_1 C_1} \tag{4.70}$$

There, we had considered three voltage input functions, namely the step function, the linear rise function and the exponential rise functions. The linear rise function was not considered further because its output did not resemble the experimental curves. The remaining two input functions are discussed here.

1. Step Function

The current generator producing this input voltage across the parallel combination of R_1 and C_1 is, from (4.69), found to be:

$$i_i(t) = \mathcal{L}^{-1}\left[E_i C_1 \frac{(s+a)}{s}\right] \tag{4.71}$$

$$i_i(t) = E_i C_1 \delta(t) + E_i C_1 a\, u(t) \tag{4.72}$$

This equation states that the current generator consists of a DELTA function and a STEP function. From the point of view of molecular behavior, it is highly improbable that there is an infinite current flow at $t = 0$.

2. Exponential Voltage Input

Here the equation of the current generator as found from (4.69) again is,

$$i_i(t) = E_i \alpha C_1 \left(\frac{a}{\alpha} + \frac{\alpha - a}{\alpha} e^{-\alpha t} \right) \qquad (4.73)$$

When this function is plotted, we have the curve in Fig. 4.12.

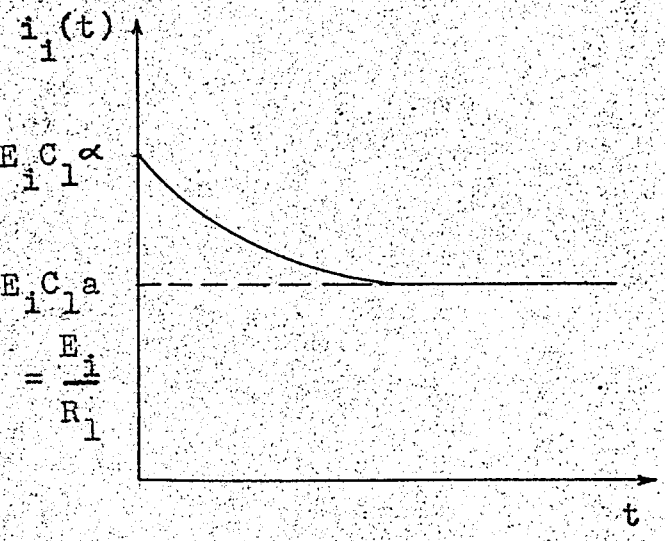

Fig. 4.12

This curve reveals that as the odor molecules reach the detector surface at $t = 0$ current starts to decrease from a predetermined value, which depends on the type of odorant to a constant final value independent of the odorant but is bound to the dielectric resistance, R_1.

Although the above current generator is not valid for acetone as has been previously discussed in detail, it can provide an answer to the responses obtained with other odorants.

II. Current Input Functions:

As has been mentioned earlier, current input functions were considered specifically to find a proper input for acetone, and

it was found that an exponential current decay with a nonzero final value could be an answer for the case of acetone.

Fig. 4.13 (a) and (b) illustrate the charge and current functions of this input.

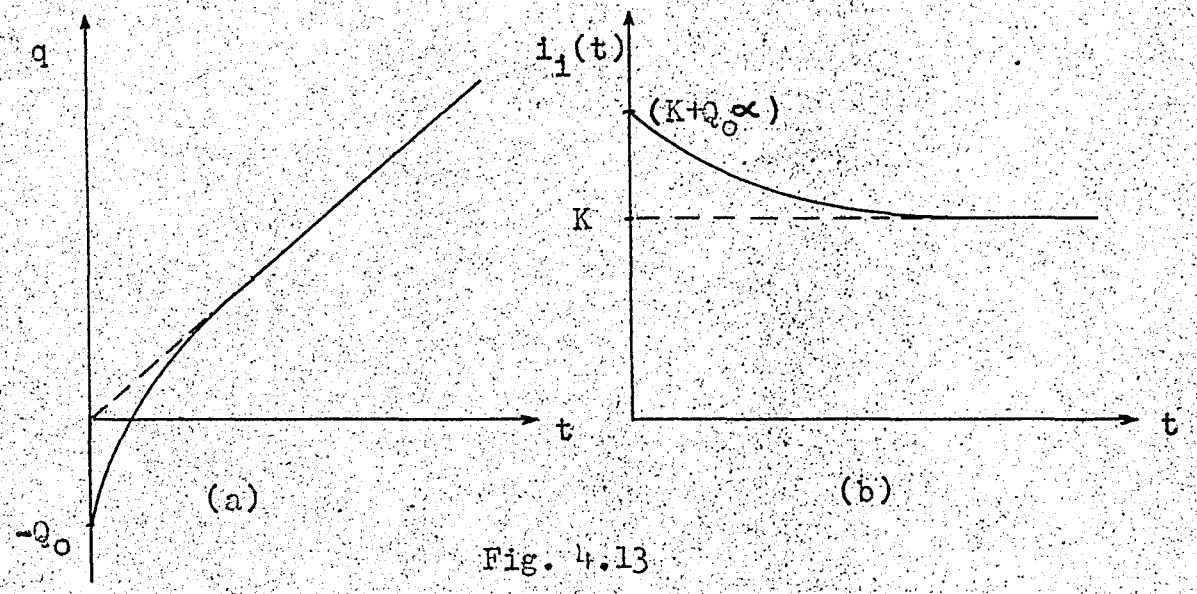

Fig. 4.13

It is seen from these curves that for large values of t, the charge is a linear function of time and current assumes a constant value. When Fig. 4.12 and Fig. 4.13(b) are compared, it is seen that the current functions have essentially the same form. In fact, the input producing the output of Fig. 4.12, that is, the voltage input function $E_1(1 - e^{-\alpha t})$ is only a special case of the more general equivalent voltage generator of the current generator considered in Section 4.6 for acetone. For if we convert the current generator of Equation 4.59 to an equivalent voltage generator to which the parallel combination of R_1 and C_1 are connected in series, we have;

$$e_i(t) = \frac{K}{rC_1}\left[\frac{r}{a} + \frac{(r-\alpha)}{(\alpha-a)}e^{-\alpha t} + \frac{(a-r)}{a(\alpha-a)}e^{-at}\right] \qquad (4.74)$$

If we consider the special case in which $r = a > b$ (4.74) reduces to:

$$e_i(t) = \frac{K}{rC_1}\left(1 - e^{-\alpha t}\right) \qquad \text{or,}$$

$$e_i(t) = KR_1\left(1 - e^{-\alpha t}\right) \tag{4.75}$$

where KR_1 can be called E_i. Therefore, if the conditions of charge build-up are such that; $a = r$ or

$$\frac{K\alpha}{K + Q_0\alpha} = \frac{1}{R_1C_1} \tag{4.76}$$

we have the output responses which can be represented by (4.25) and having the plots in Fig. 4.1a.

For acetone, however, since we want to get a curve like that of Fig. 4.1b, and also require that $a > b$, the above special case does not hold; and the voltage input function has to retain its general form in (4.74).

Finally, it remains for this discussion to investigate whether the evaluated constants of 4.63 agree with the implications of our measurements discussed in the previous chapter.

We know that the input resistance and capacitance of the measuring device are constant and have the maghitudes of orders 10^{14} ohms and 22pF respectively. We also assume that the detector capacitance does not change very much. From the measurement this capacitance was found to be 220 pF. If we take here a value around 200 pF, to account for some change after the application of the odorant to the detector, from;

$$b = \frac{R_1 + R_2}{R_1 R_2 (C_1 + C_2)} \qquad (4.77)$$

we find that R_1 is a resistance of the order 10^{10} ohms.

From the measurements of Chapter III, R_1 was found to be 10^9 ohms. Therefore, the above two values can be considered to be in agreement.

CHAPTER V

CONCLUSION

In the previous four chapters of this report, beginning with a detailed description of the Electro-Odocell and the responses obtained from it as it is coupled to the measuring device, we have considered a possible electrical equivalent circuit of the system based on the general output characteristics of some odorants. Emphasis was given to the acetone response, as most of the odorants tested gave curves of similar shape.

The assumed equivalent circuit as developed in Chapter IV is illustrated here once more by Fig. 5.1.

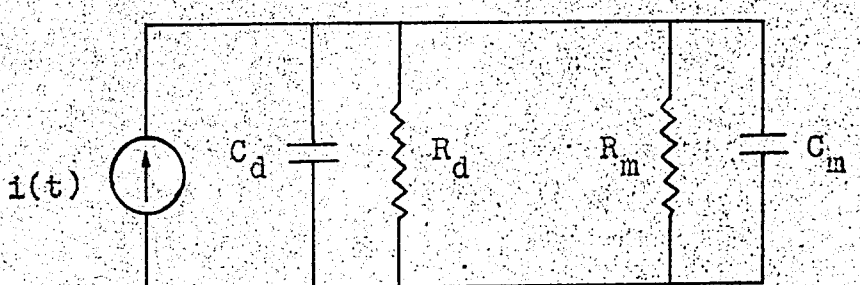

Fig. 5.1

In Chapter II, the general characteristics of output functions, the input characteristics of the measuring device and the ideal representation of a dielectric in terms of network parameters were given.

Based on such a representation of a dielectric material, the parameters R and C of the Electro-Odocell (EOC) were considered in Chapter III.

Because of the geometry and construction of the Electro-

Odocell, it was first assumed that the resistance associated with the dielectric of the EOC consisted of a s u r f a c e and a v o l u m e resistance component. This assumption was soon abandoned as a result of several measurements in which both surface and volume resistance components were investigated.

The main conclusions of Chapter III pertaining to the detector dielectric resistance can be summarized as follows:

1. Total resistance does not include a surface dielectric resistance and its order seems to be between 10^9 - 10^{11} ohms.
2. The resistance is bilateral and changes with humidity (i.e. it decreases as humidity increases). It also changes with the pressure applied to it by the transducer cap (i.e. decreases with increasing pressure).

The rest of Chapter III dealt with the second important element of the dielectric; its capacitance. The results of experiments in that section led us to the following conclusions:

1. Capacitance increases with increasing effective dielectric area and with decreasing dielectric thickness.
2. Capacitance also changes with applied pressure on the dielectric (i.e. increases with increasing pressure).
3. When mica is used in the detector as the dielectric, the main variable seems to be the capacitance.

Finally in Chapter IV, we considered the equivalent circuit and the responses of the detector together, in an effort to find an input function which would produce the desired output

characteristics.

Several voltage and current input functions were considered with the proper transfer function of the equivalent circuit in each case. As a result of these investigations, it was found that a voltage generator, having the general form shown in 5.1 and an internal impedance consisting of the dielectric resistance R_1 (or R_d) connected in parallel with the dielectric capacitance C_1 (or C_d), could be considered as the input to the equivalent circuit.

$$e_i(t) = \frac{K}{rC_1}\left[\frac{r}{a} + \frac{(r-\alpha)}{(\alpha-a)}e^{-\alpha t} + \frac{\alpha(a-r)}{a(\alpha-a)}e^{-at}\right] \qquad (5.1)$$

The constants K, r and α in this equation are associated with the odorant and a with the internal impedance of R_1, C_1 in parallel.

Equation 5.1 in its general form provided an answer as the input function of the acetone response, as illustrated in Fig. 4.1b, whereas its special case in which $a = r$ provided an answer as the input function of the other odorant responses in Fig. 4.1a.

The equivalent current generator and, therefore, the charge generator equations of the input voltage represented by Equation 5.1 were also disucssed and their graphs were illustrated in Section 4.7.

As the concluding observations and considerations of this chapter a few more paragraphs may be added concerning the behavior of the simulated acetone response in the laboratory.

When the assumed equivalent circuit and the input function for acetone were simulated in the laboratory, the changes noted below were observed in the response by varying the network elements:

1. R_1 changed, C_1 kept constant.

   When R_1 is increased, final value increases and the shape of the output changes from (1) to (2) in Fig. 5.2.

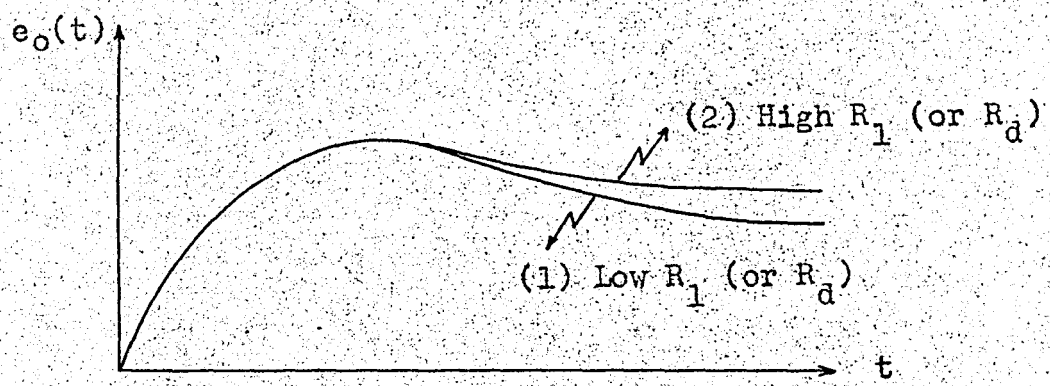

Fig. 5.2

2. C_1 changed, R_1 kept constant.

   When C_1 is increased both initial slope and final value decrease, and the shape of the curve changes from (1) to (2) in Fig. 5.3.

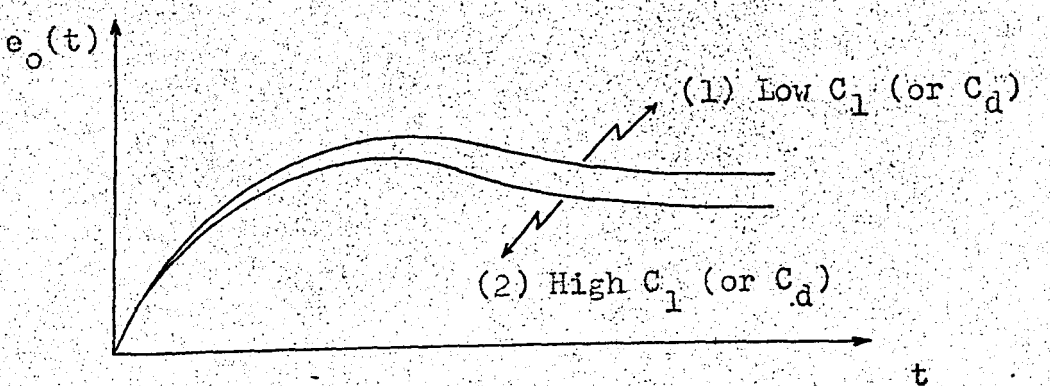

Fig. 5.3

Therefore, if the equivalent circuit we have adopted and the input functions we have considered provide a fair representation of the odor detection phenomenon, the following requirements must be met for a large steady state value with a fast speed of response.

1. For a large steady state value detectors having large dielectric resistance and low capacitance must be selected.
2. For a fast speed of response capacitance must be low.

However, the experiments , in which the values of detector parameters in relation to the final value and the speed of response of the output were investigated, showed that the capacitance had to be large as well as the resistance for optimum response. Therefore, it is suggested that further investigations be carried out along this line.

Once the detectors with the most desired properties can be constructed, research may be directed to the investigation of the physico-chemical phenomena causing the potential build-up across the dielectric surfaces.

APPENDICES

APPENDIX II

Acetone Response:

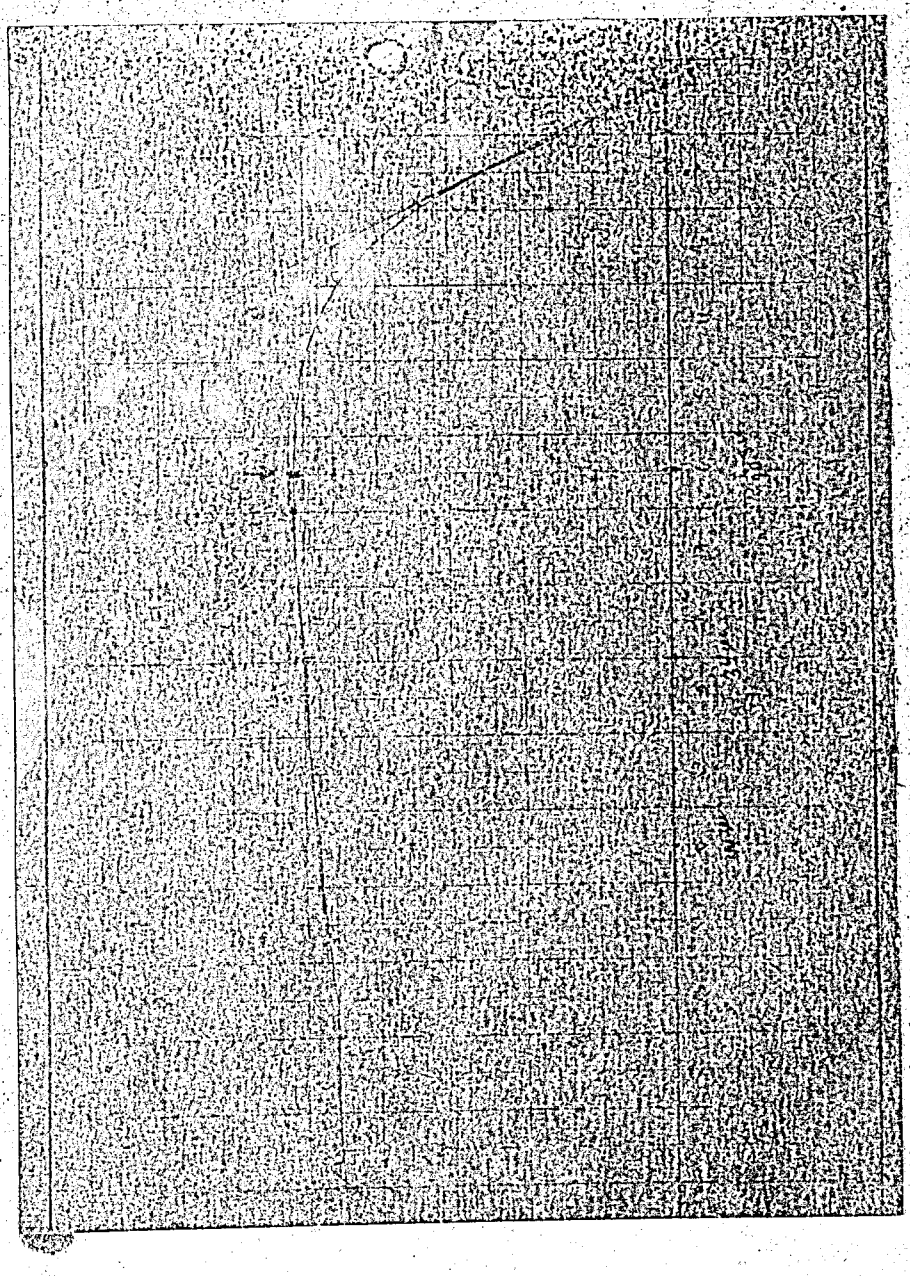

APPENDIX III A

A. Determination of Dielectric Resistivities:

Measured current (in amperes) through specimen at 480 volts						
Dielectric	Clean mica $t=12.7\times10^{-3}$ cm		Dotted mica $t=7.6\times10^{-3}$ cm		Paper $t=19\times10^{-3}$ cm	
No of Meas.	Vol.Res	Surf.Res	Vol.Res.	Surf.Res.	Vol.Res.	Surf. Res.
1	1.00×10^{-9}	4.00×10^{-8}	3.00×10^{-9}	1.50×10^{-9}	4.50×10^{-6}	1.00×10^{-7}
2	0.80×10^{-9}	4.50×10^{-8}	2.00×10^{-9}	2.00×10^{-9}	2.50×10^{-6}	1.00×10^{-7}
3	3.00×10^{-9}	5.00×10^{-8}	5.00×10^{-9}	0.80×10^{-9}	1.80×10^{-6}	0.80×10^{-7}
4	4.00×10^{-9}	2.50×10^{-8}	8.00×10^{-9}	9.00×10^{-9}	2.50×10^{-6}	0.30×10^{-7}
5	4.00×10^{-9}	3.00×10^{-8}	10.00×10^{-9}	5.00×10^{-9}	4.50×10^{-6}	0.90×10^{-7}
6	5.00×10^{-9}	4.00×10^{-8}	2.00×10^{-9}	2.50×10^{-9}	3.50×10^{-6}	1.10×10^{-7}
7	1.10×10^{-9}	4.60×10^{-8}	10.00×10^{-9}	4.50×10^{-9}	5.00×10^{-6}	1.50×10^{-7}
8	0.70×10^{-9}	5.00×10^{-8}	10.00×10^{-9}	3.50×10^{-9}	3.50×10^{-6}	0.75×10^{-7}
Mean	2.40×10^{-9}	4.00×10^{-8}	8.50×10^{-9}	3.50×10^{-9}	3.40×10^{-6}	0.92×10^{-7}

CALCULATIONS:

Electrode dimensions: $D_1 = 5.08$ cm $D_2 = 5.72$ cm $g = 0.32$ cm

$D_o = (D_1 + D_2)/2 = 5.40$ cm

$P/g = \pi D_o/g = 53.4$

Effective Areas (A) in Equation (3.3)

Clean mica : 20.38 sqcm

Dotted mica: 20.20 sqcm

Paper : 20.38 sqcm

Volume Resistivities (ρ). From $\rho = A.R/t$ ohm.cm

Clean mica : 3.20×10^{14} ohm.cm

Dotted mica: 1.52×10^{14} "

Paper : 1.51×10^{11} "

Surface Resistivities (σ). From $\sigma = P.R/g$ ohms.

Clean mica : 6.40×10^{11} ohms

Dotted mica: 7.30×10^{12} "

Paper : 2.78×10^{11} "

B. Volume Resistance (R_V) : From (3.8) A = 1.30 sqcm

Clean mica : 5.12×10^{12} ohms

Dotted mica: 0.89×10^{12} "

Paper : 2.78×10^{8} "

C. Surface Resistance (R_S). From (3.9)

Clean mica : 2.04×10^{11} ohms

Dotted mica: 2.22×10^{12} "

Paper : 0.88×10^{11} "

D. Total Dielectric Resistance (R). From $R = R_V.R_S/(R_V + R_S)$

Clean mica : approx. 10^{11} ohms

Dotted mica: " 10^{11} "

Paper : " 10^{11} "

E. Results of Voltmeter-Ammeter Method:

Clean mica : 10^{9} ohms

Dotted mica: 10^{9} "

Paper : 10^{9} "

APPENDIX III B

Effects of Dielectric Material and Detector Cap Area:

TABLE B1

Increasing cap area	Mica		Paper	
	C_p(pF)	D	C_p(pF)	D
1	225	0.028	186	0.042
2	255	0.028	190	0.042
3	231	0.030	191	0.042
4	231	0.028	191	0.042

Effect of Dielectric Thickness:

TABLE B2

Thickness (10^{-3} cm)	MICA			
	Sample A		Sample B	
	Capacitance (pF)	D	Capacitance (pF)	D
3.56			234	0.021
(*) 3.80			231	0.030
5.08	234	0.02	223	0.020
7.62	225	0.03	203	0.014

(*) When this sample was squeezed it was found that the capacitance inreases to 246 pF and D increases to 0.053. This is in accordance with the theoretical predictions. The increase in capacitance means decrease in thickness by increased pressure and the increase in D means decrease in resistance, since

$$R_p = 1/wC_pD \quad \text{and} \quad C_p = K.S/d$$

where: S = capacitor plate area, t = dielectric thickness

K = a proportionality constant

The effects of thickness and detector cap area are illustrated in the below table

TABLE B3

Thickness (10^{-3}cm)	PAPER			
	Smaller Cap area		Large Cap area	
	C_p(pF)	D	C_p(pF)	D
17.8	176	0.026	195	0.046
35.6	168	0.024	175	0.026
53.4	164	0.020		

Tables B1, B2 and B3 are also plotted on the following pages to show the inverse relationships more clearly.

APPENDIX IIIC

Plots of measurements

GRAPH Ia

Detector no: 4 with MICA

RH: % 54

(—) term. at supply

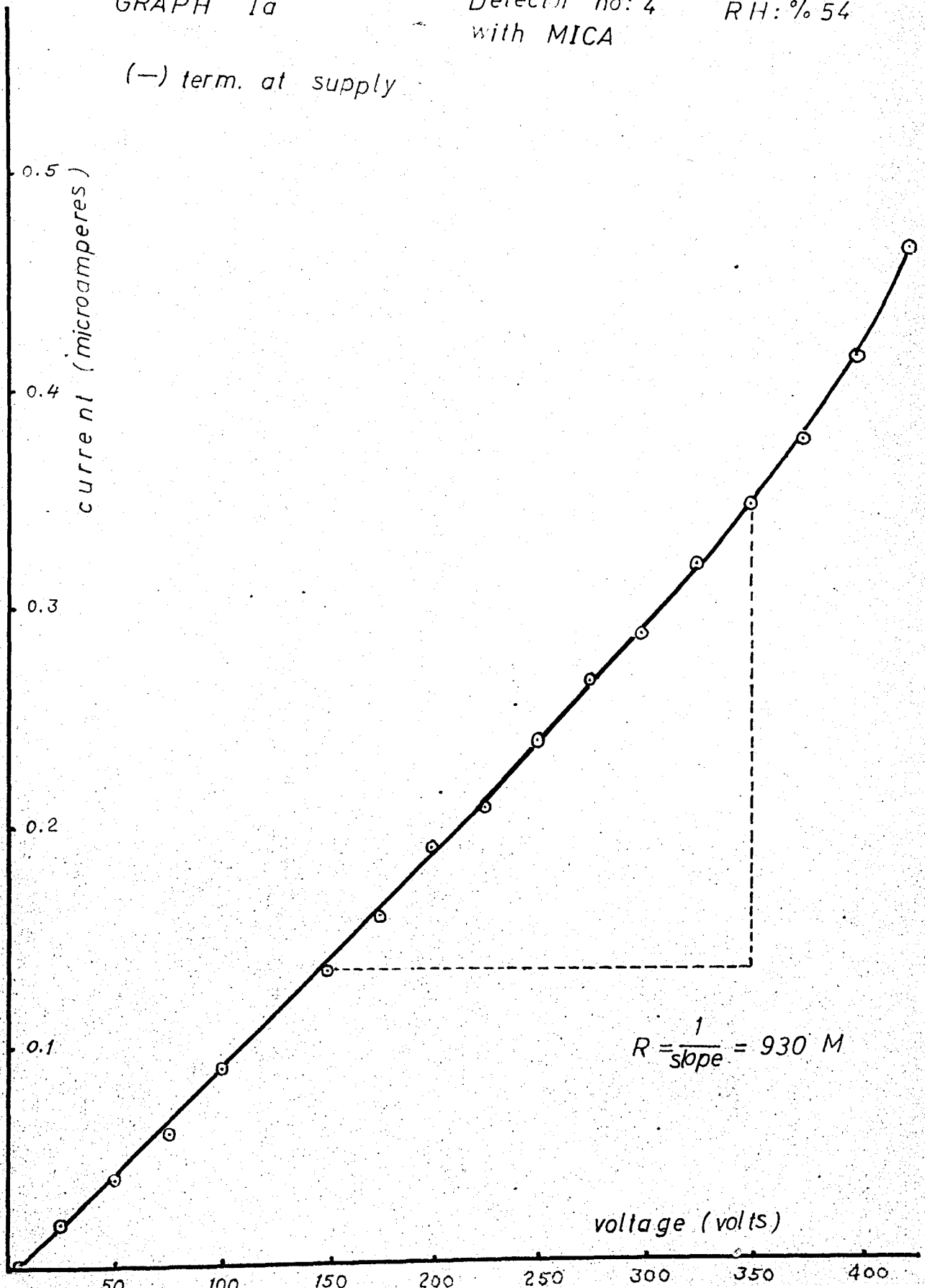

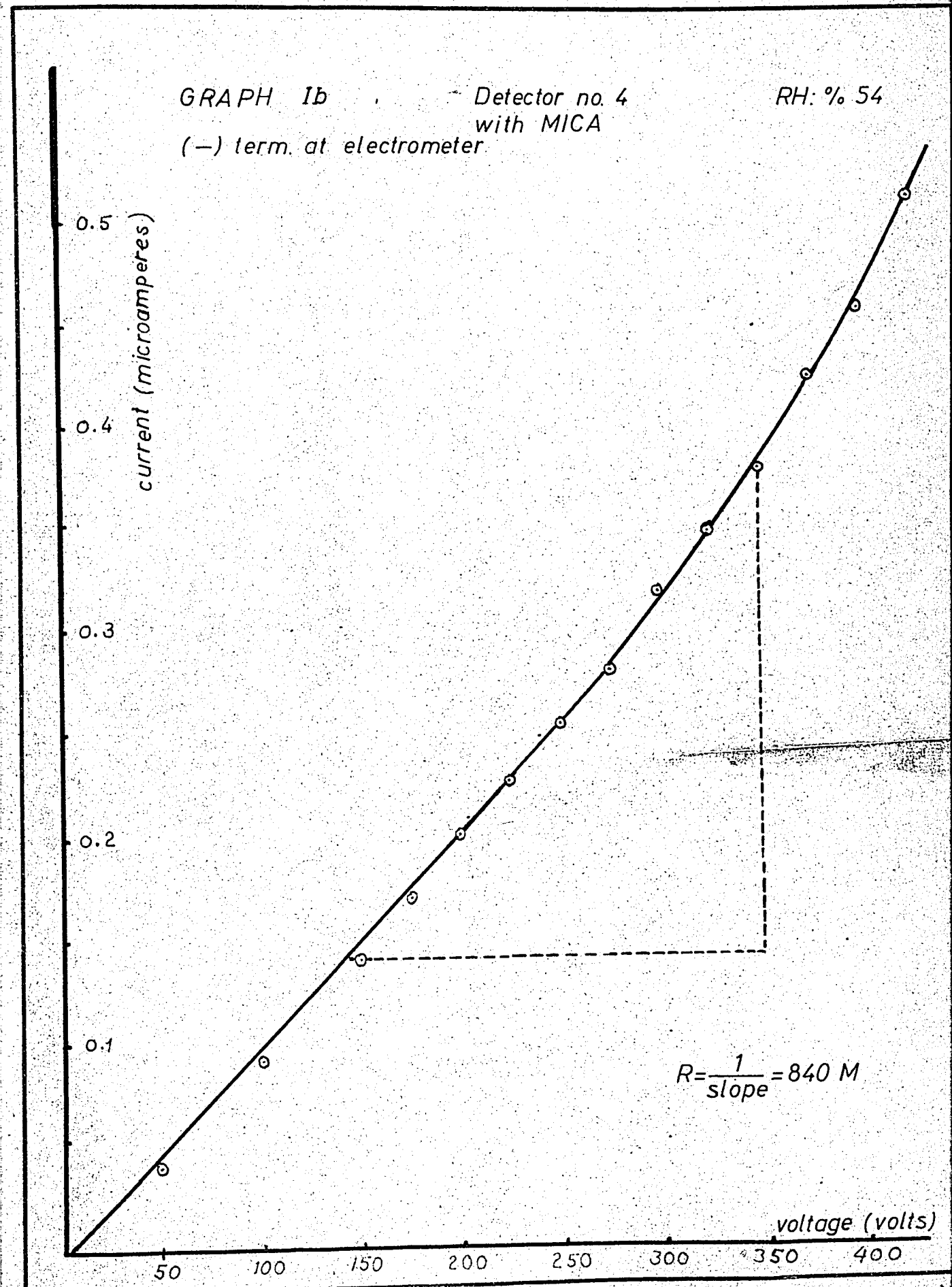
GRAPH Ib
Detector no. 4
with MICA
RH: % 54
(−) term. at electrometer
current (microamperes)
0.5
0.4
0.3
0.2
0.1
R=1/slope = 840 M
voltage (volts)
50
100
150
200
250
300
350
400

GRAPH II a

Detector no. 4
with MICA
smaller area

RH: % 54

(–) term. at supply

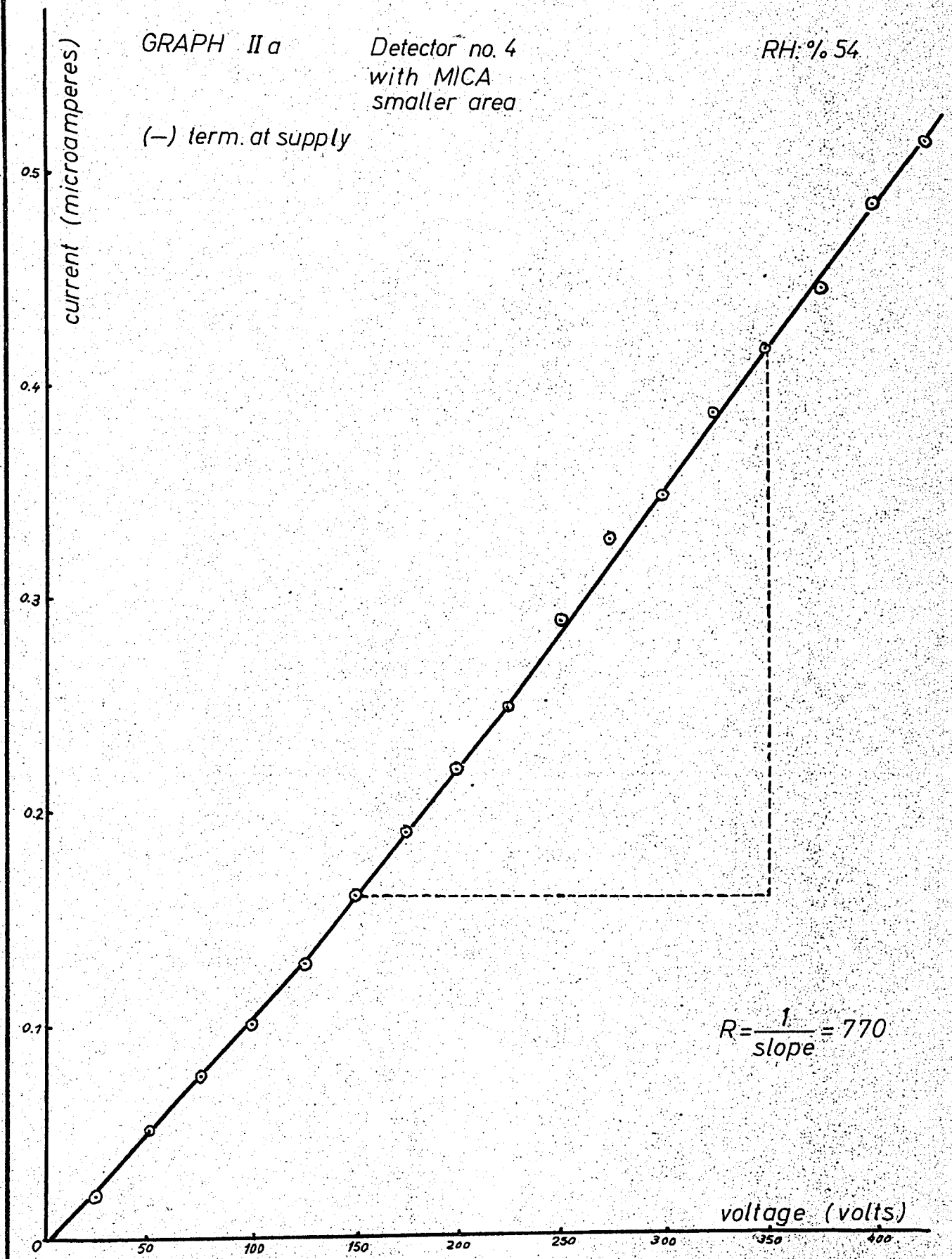

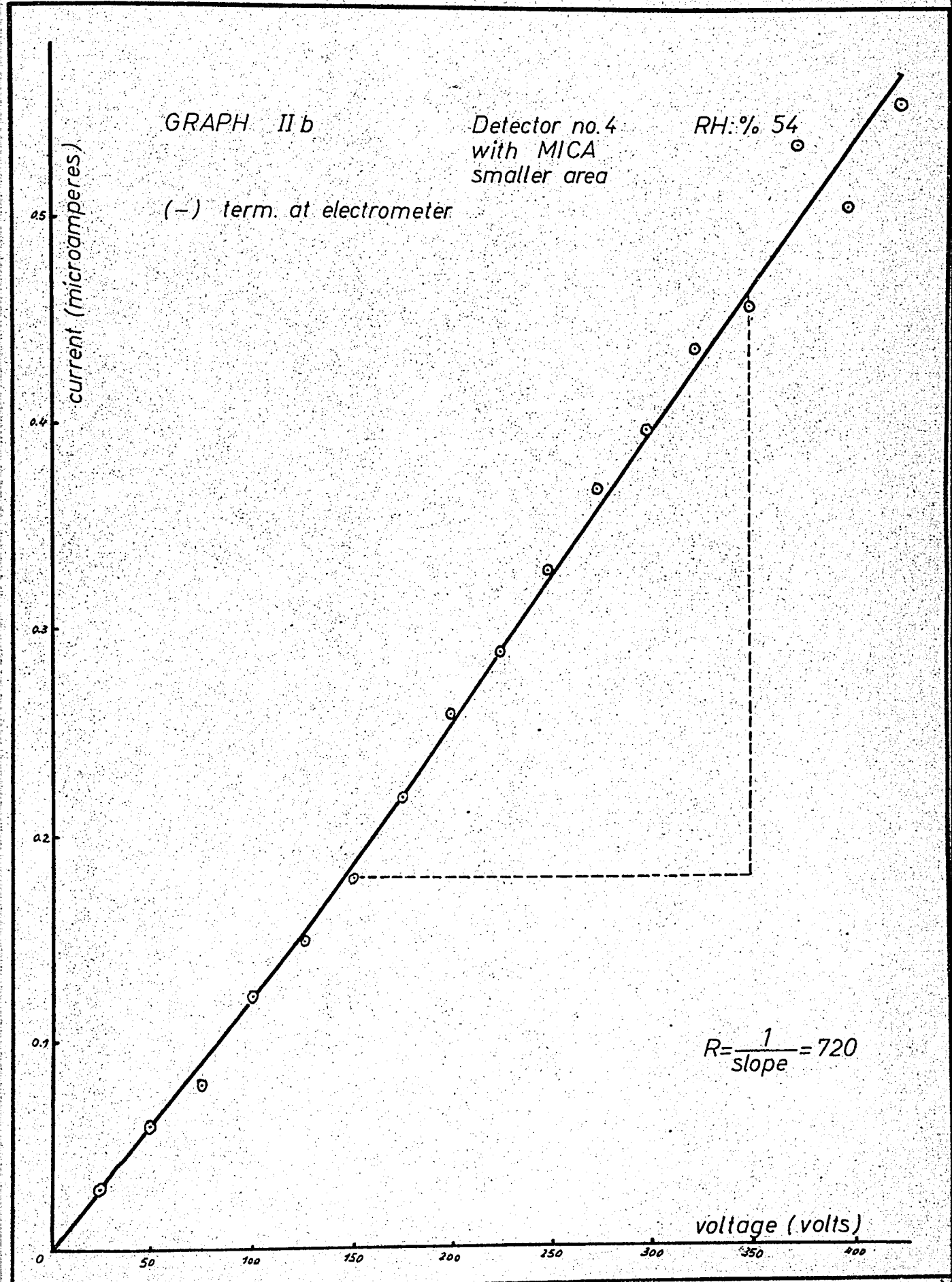
GRAPH II b
Detector no.4
with MICA
smaller area
RH: % 54
(–) term. at electrometer
current (microamperes)
0.5
0.4
0.3
0.2
0.1
0
50
100
150
200
250
300
350
400
voltage (volts)
R = 1/slope = 720

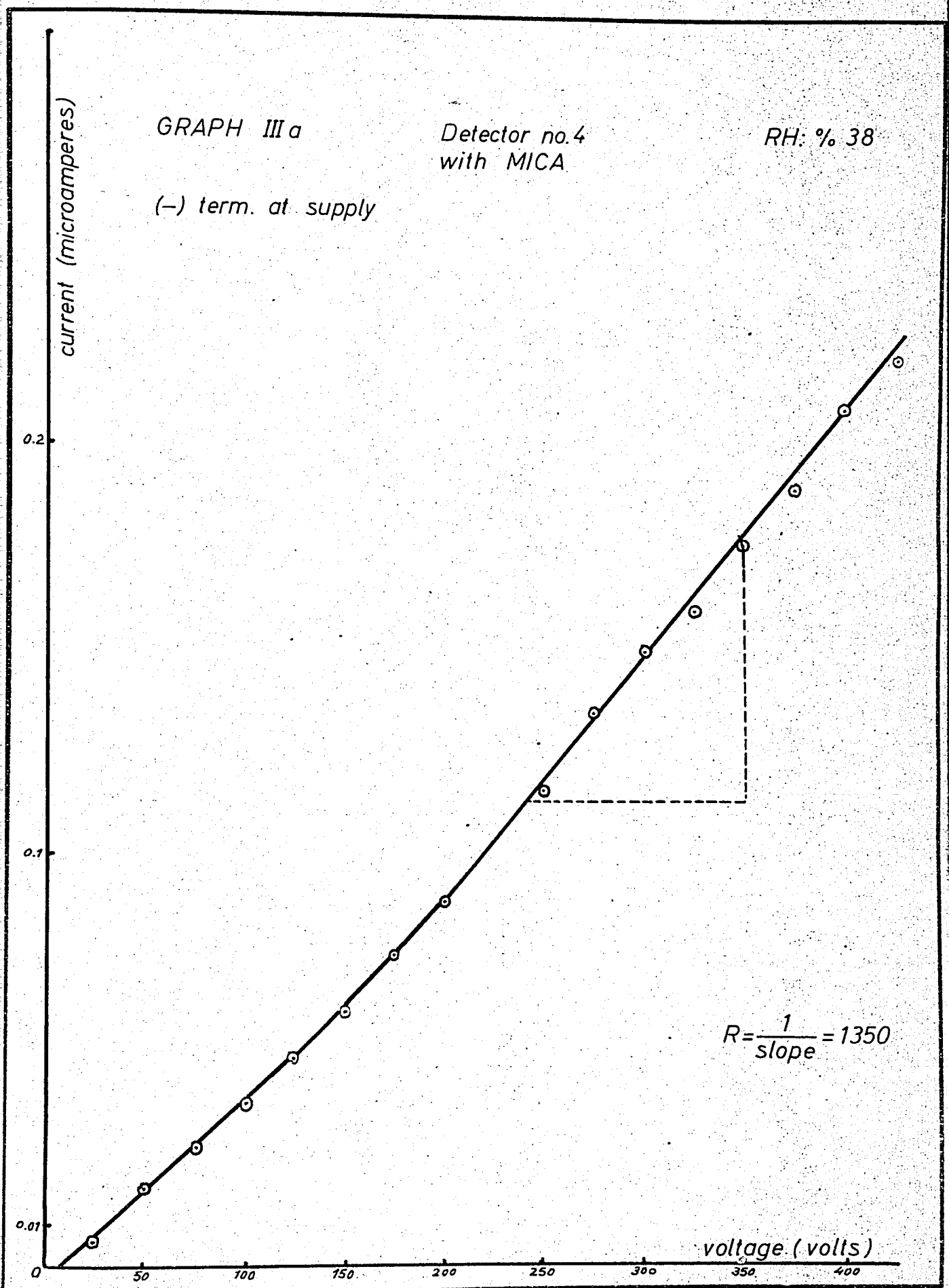
GRAPH III a
Detector no.4
with MICA
RH: % 38
(–) term. at supply
current (microamperes)
0.2
0.1
0.01
0
50
100
150
200
250
300
350
400
voltage (volts)
R = 1/slope = 1350

GRAPH no. III b

Detector no.4
with MICA

RH: % 38

(–) term. at electrometer

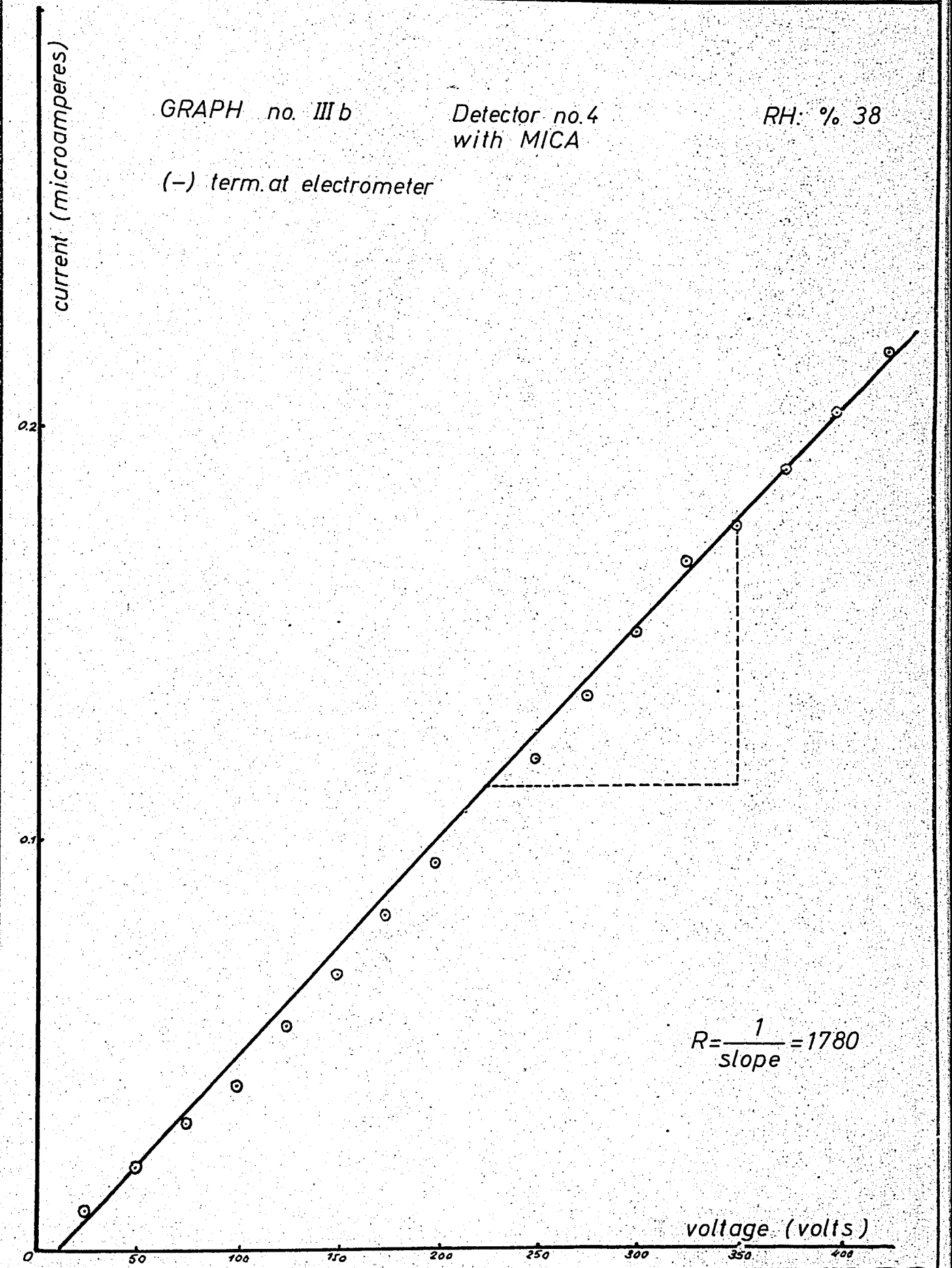

GRAPH IV a

Detector no. 4
with PAPER

RH: % 38

(–) term. at supply

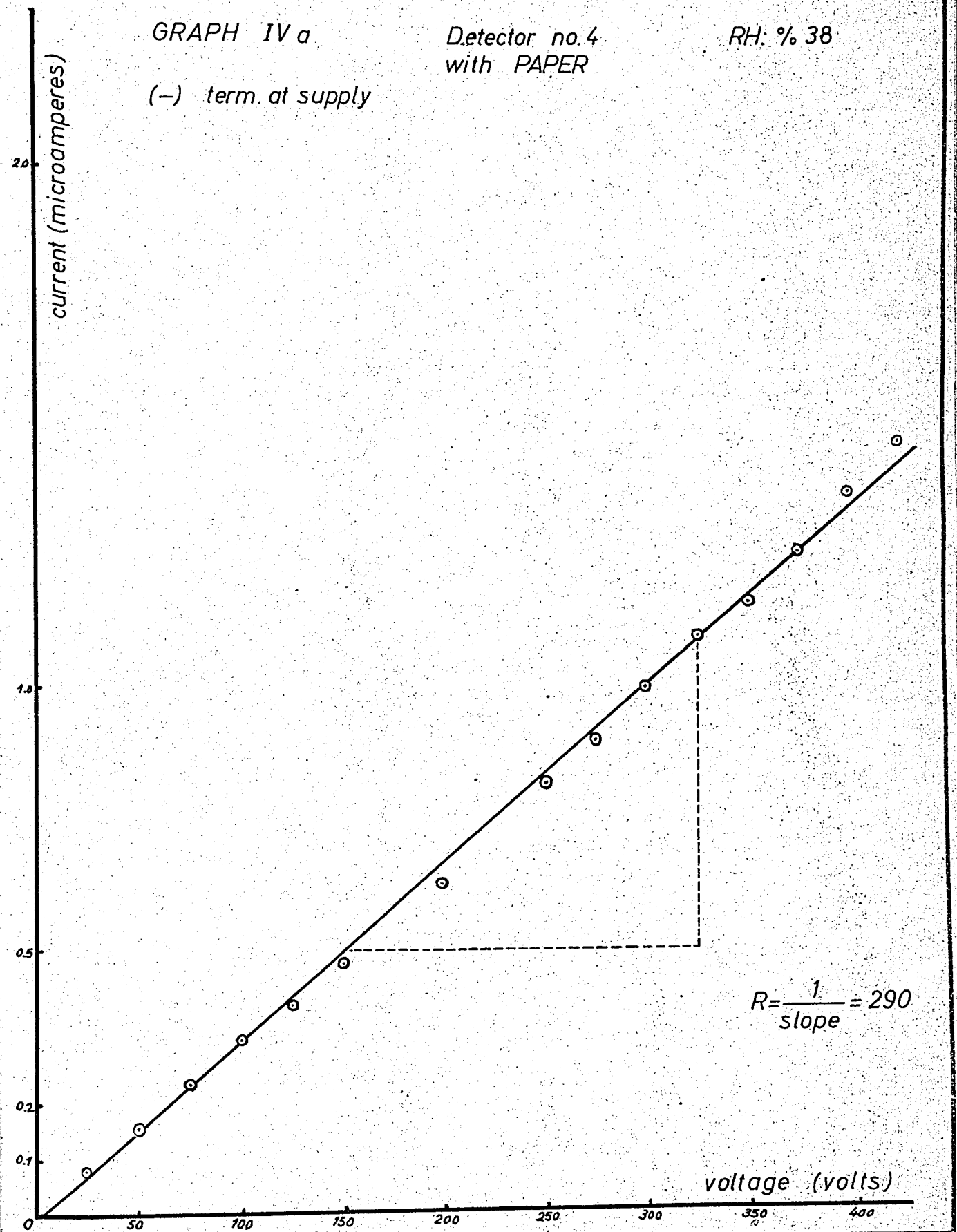

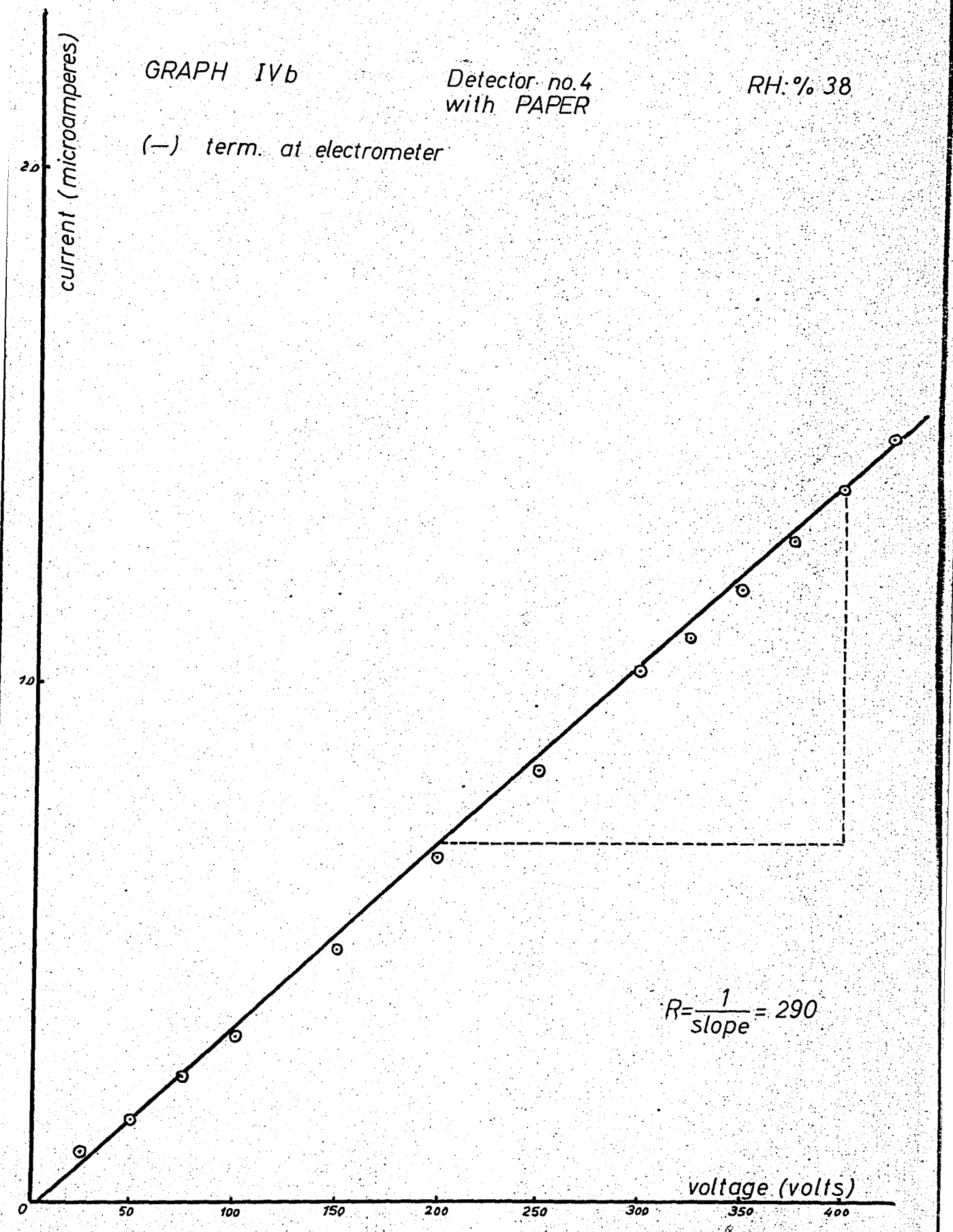
GRAPH IVb
Detector no.4
with PAPER
RH: % 38
(—) term. at electrometer
current (microamperes)
20
10
0
50
100
150
200
250
300
350
400
voltage (volts)
$R = \frac{1}{slope} = 290$

GRAPH V

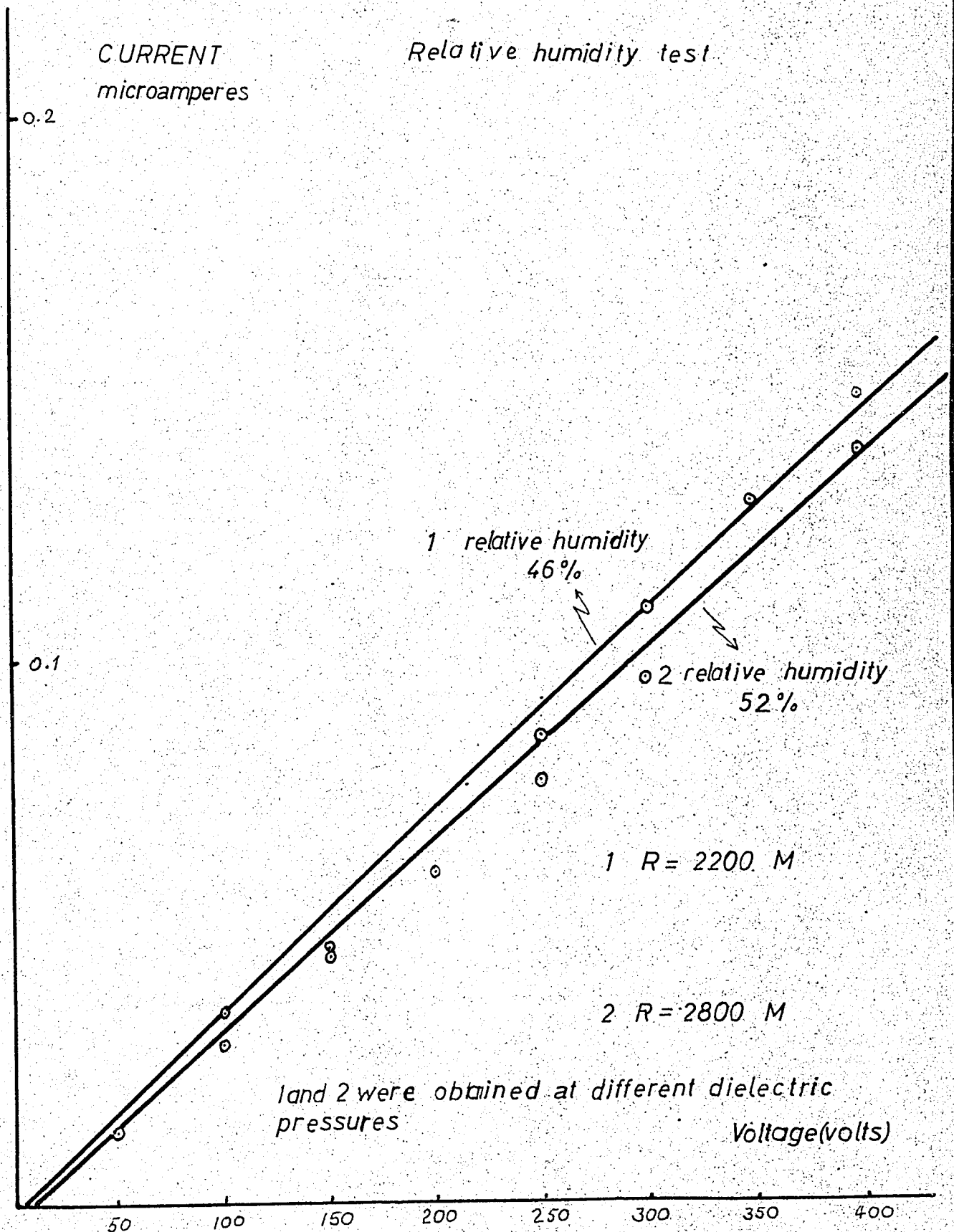
CURRENT
microamperes
Relative humidity test
0.2
0.1
1 relative humidity
46%
2 relative humidity
52%
1 R = 2200 M
2 R = 2800 M
1 and 2 were obtained at different dielectric pressures
Voltage(volts)
50
100
150
200
250
300
350
400

GRAPH VI

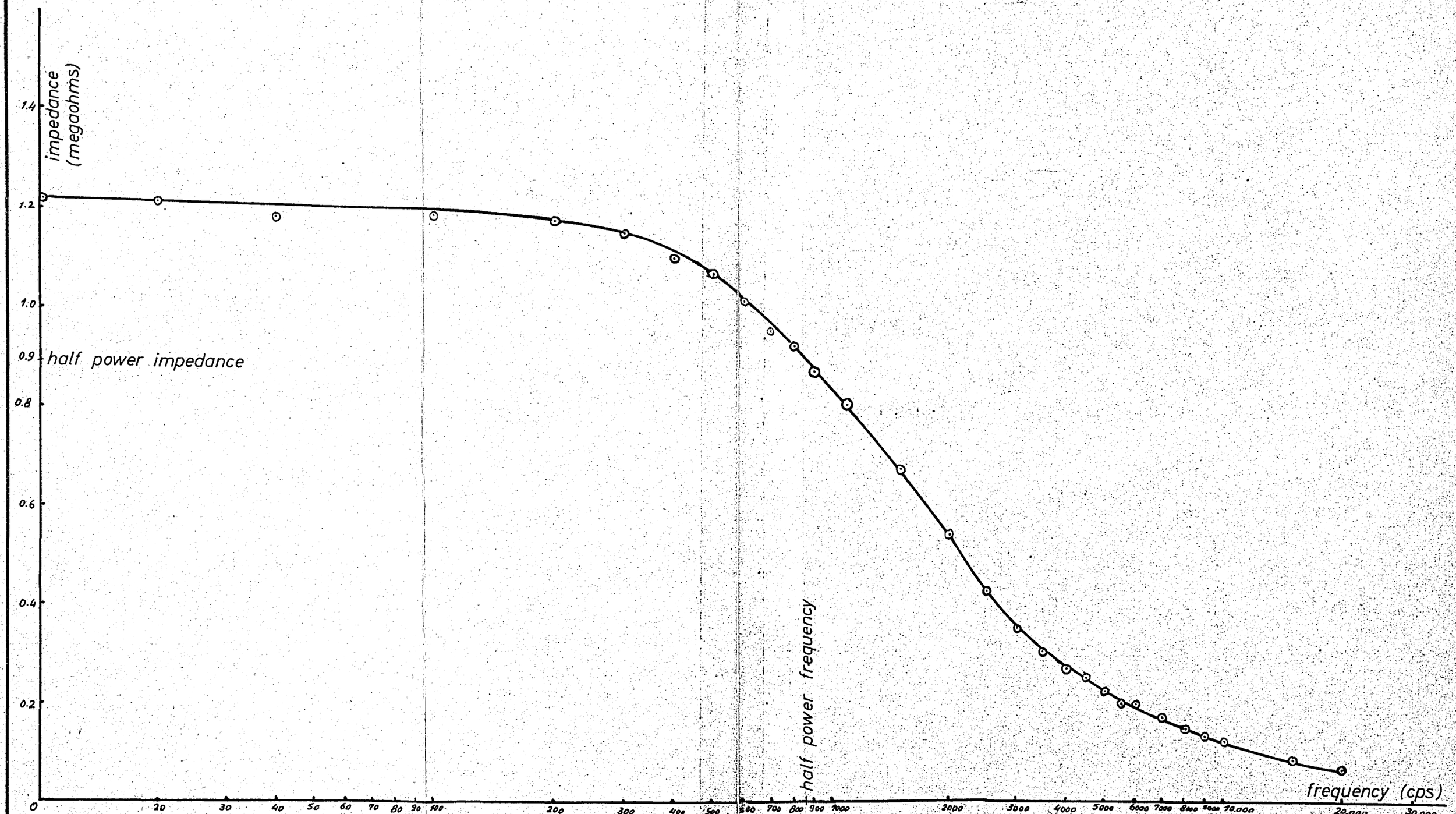
impedance (megaohms)
1.4
1.2
1.0
0.9
half power impedance
0.8
0.6
0.4
0.2
0
20
30
40
50
60
70
80
90
100
200
300
400
500
half power frequency
frequency (cps)
1000
2000
3000
4000
5000
6000
7000
8000
9000
10,000
20,000
30,000

GRAPH VII

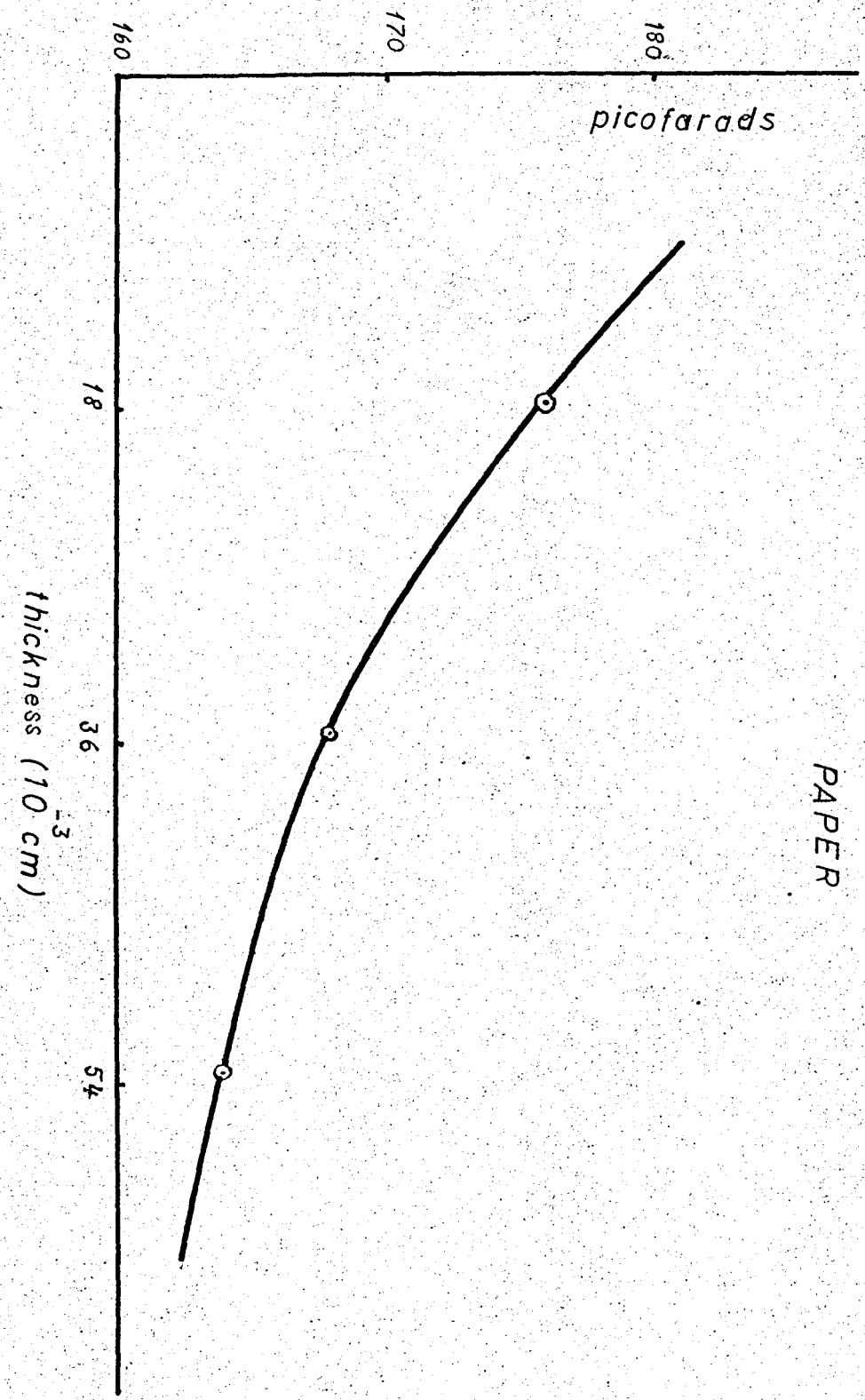

GRAPH VIII

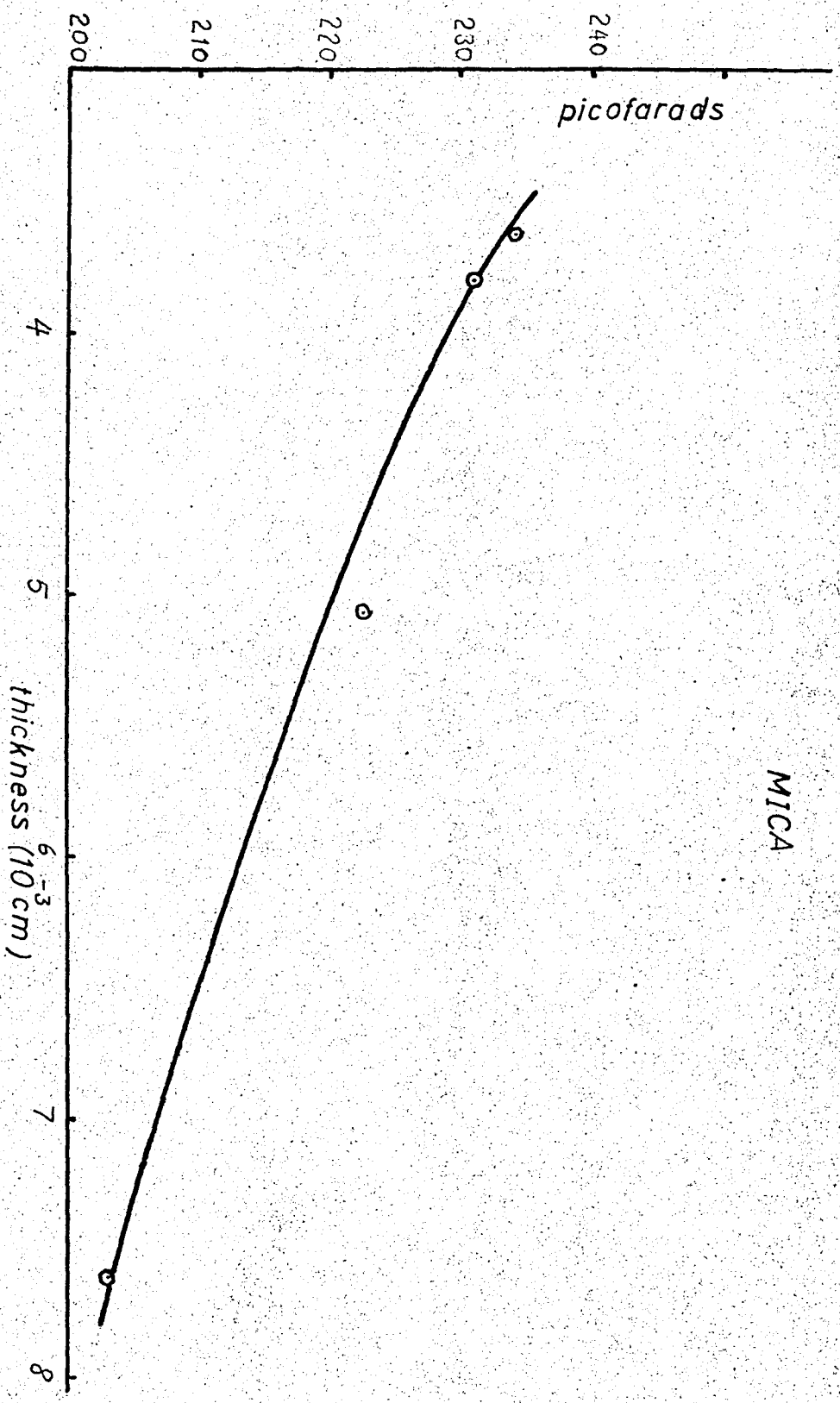

APPENDIX IV

GRAPH I

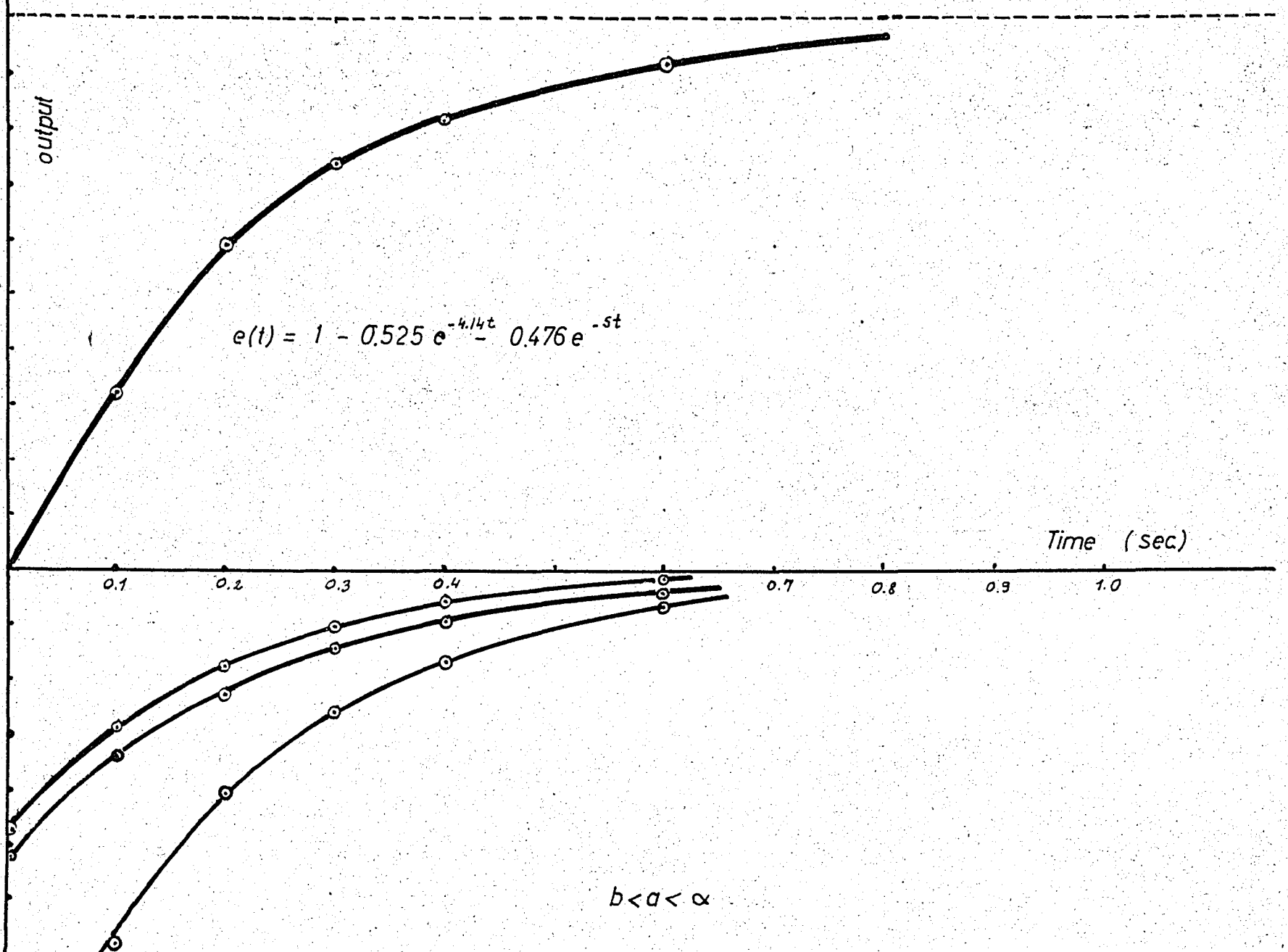

THESIS
ROBERT COLLEGE GRADUATE SCHOOL
BEBEK, ISTANBUL

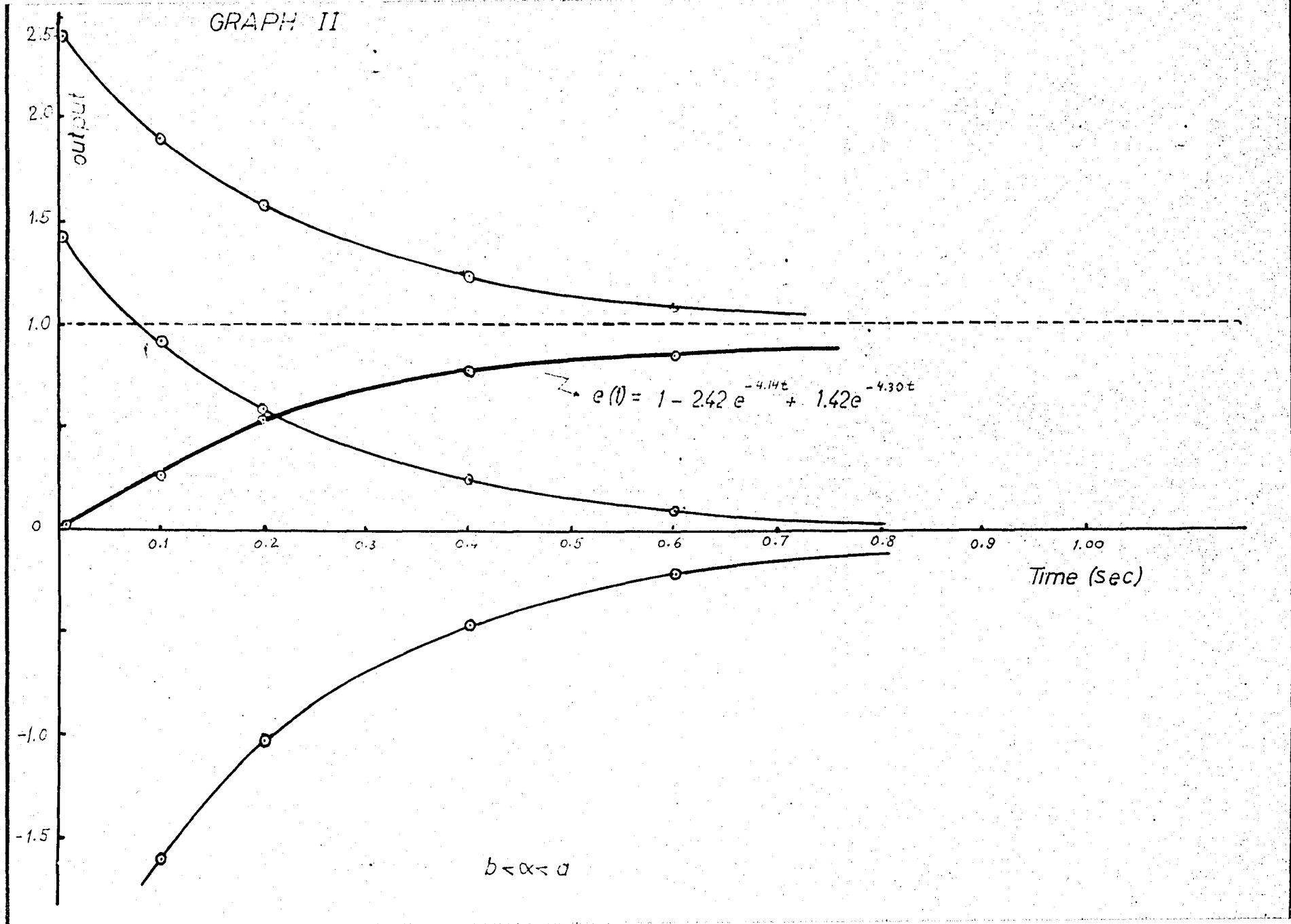

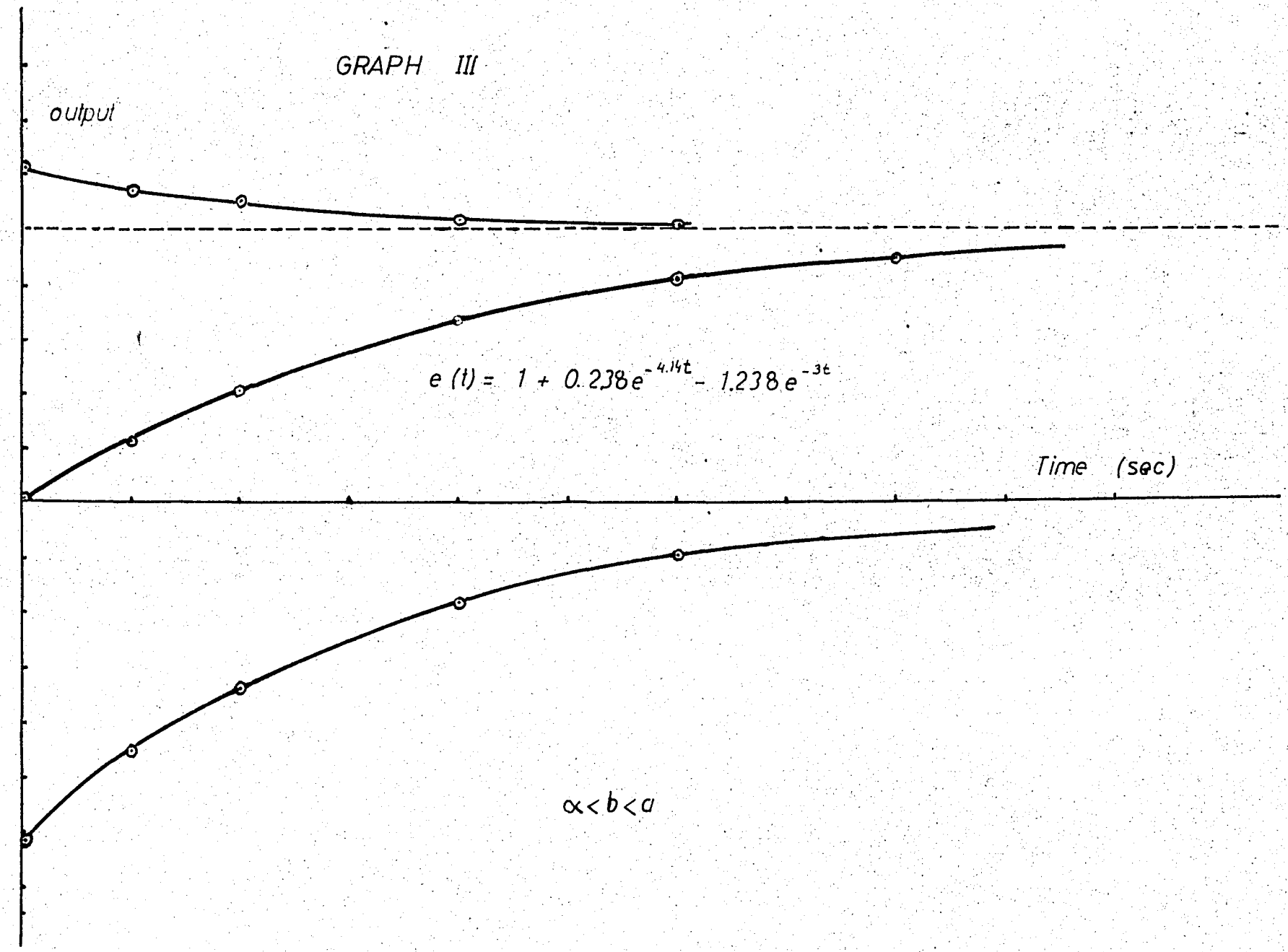

GRAPH IV

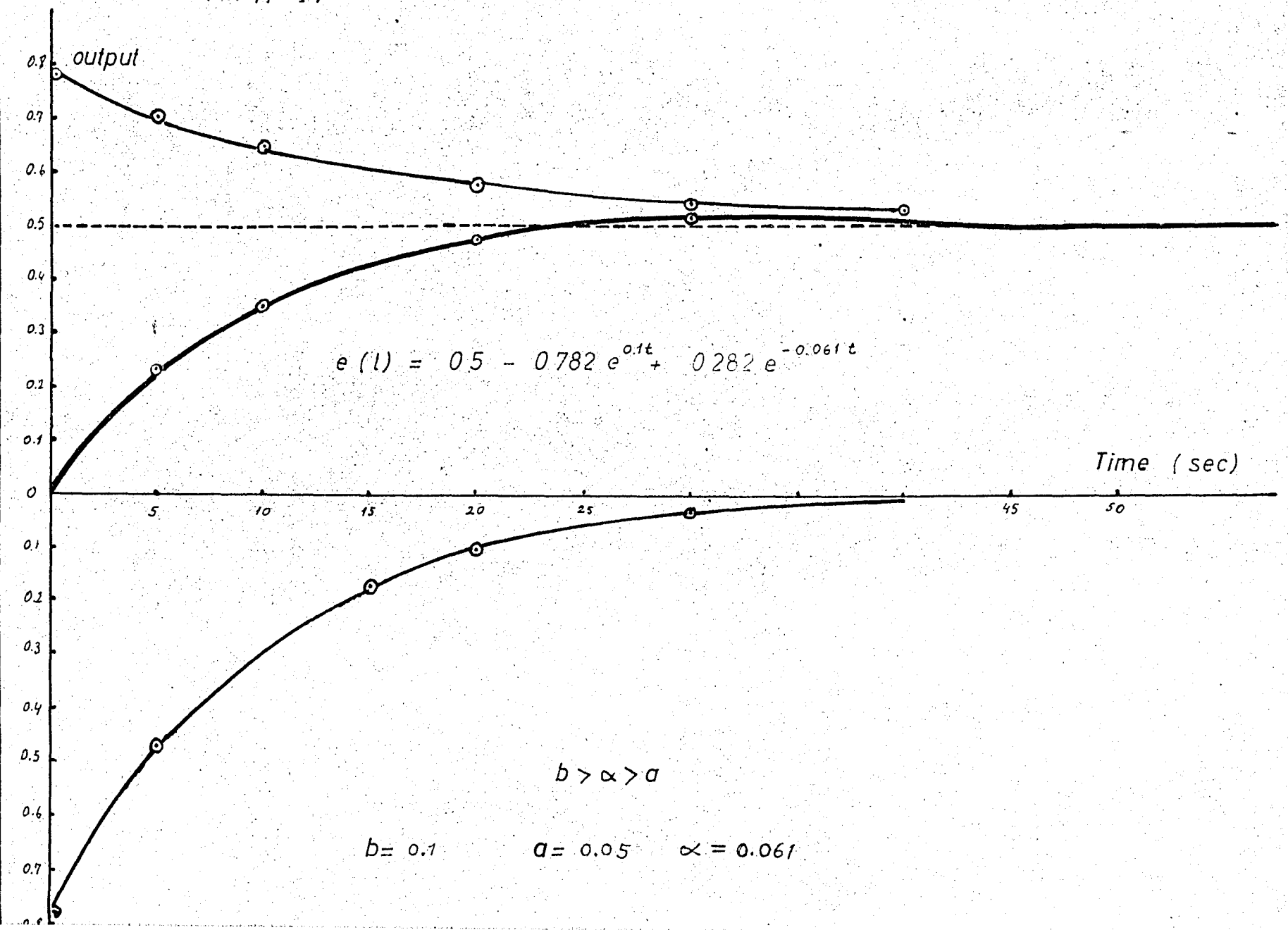

GRAPH V

comparison of representative equations
with the actual response for acetone

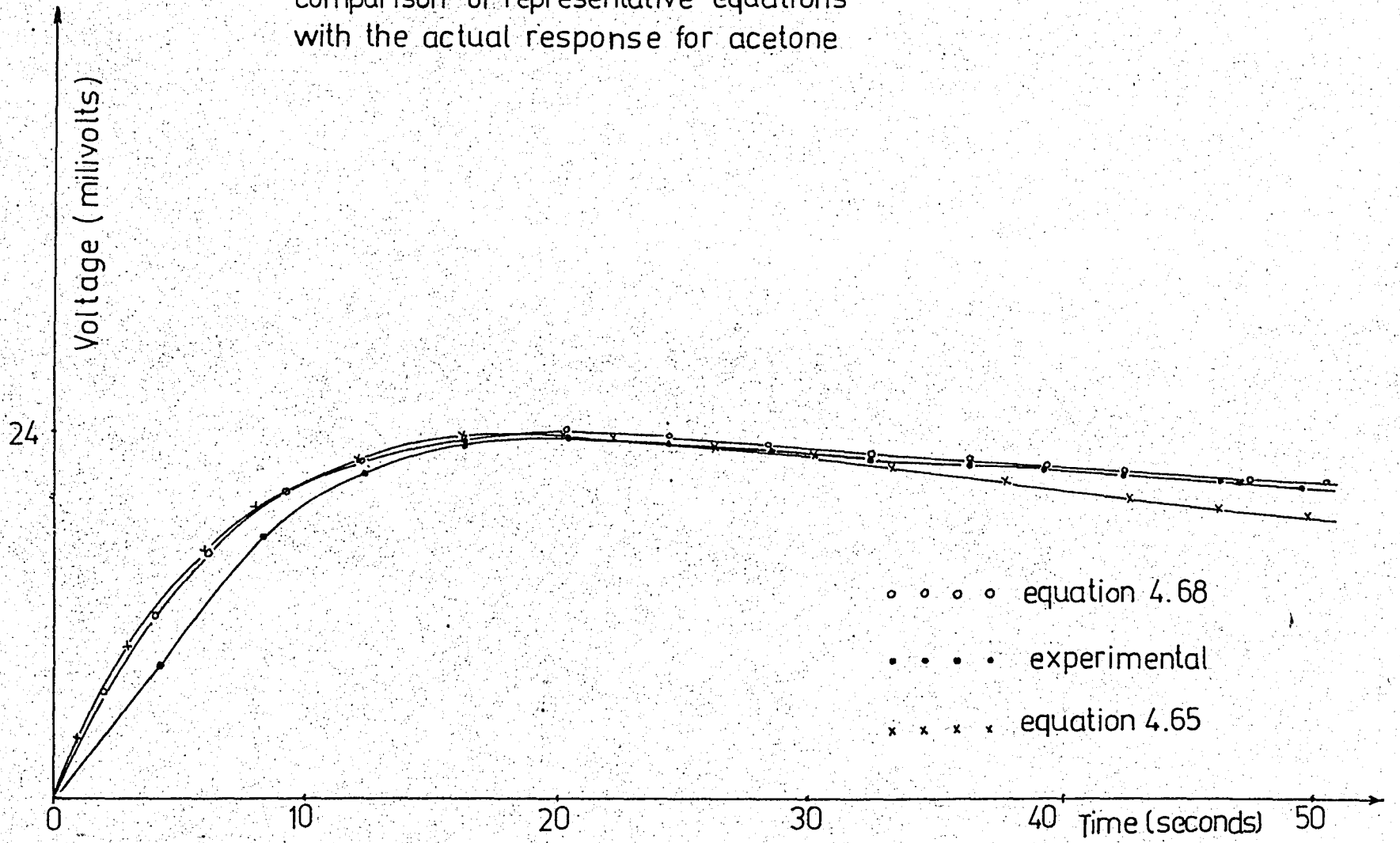

SELECTED BIBLIOGRAPHY

THALER, George J., Analysis and Design of Feedback Control Systems, McGraw-Hill Book Company, Inc., New York, 1960

NIXON, Floyd E., Principles of Automatic Controls, Prentice-Hall, Inc., Englewood Cliffs N.J., 1953

PETTIT, Joseph M., Electronic Switching, Timing and Pulse Circuits, McGraw-Hill Book Company, Inc., New York 1959

CHENG, David K., Analysis of Linear Systems, Addison-Wesley Publishing Company, Inc., Reading, Mass., 1959